SYNTHESIS AND CHARACTERIZATION OF NICKEL ZINC OXIDE NANOPARTICLES AND THEIR INVESTIGATION AS WATER OXIDATION CATALYST

A THESIS SUBMITTED TO
THE GRADUATE SCHOOL OF NATURAL AND APPLIED SCIENCES
OF
MIDDLE EAST TECHNICAL UNIVERSITY

BY

RAHİME YAĞMUR AĞCALI

IN PARTIAL FULFILLMENT OF THE REQUIREMENTS
FOR
THE DEGREE OF MASTER OF SCIENCE
IN
CHEMISTRY

SEPTEMBER 2020

Approval of the thesis:

SYNTHESIS AND CHARACTERIZATION OF NICKEL ZINC OXIDE NANOPARTICLES AND THEIR INVESTIGATION AS WATER OXIDATION CATALYST

submitted by **Rahime Yağmur Ağcalı** in partial fulfillment of the requirements for the degree of **Master of Science** i**n Chemistry, Middle East Technical University** by,

Prof. Dr. Halil Kalıpçılar
Dean, Graduate School of **Natural and Applied Sciences** _____

Prof. Dr. Cihangir Tanyeli
Head of the Department, **Chemistry** _____

Prof. Dr. Emren Nalbant Esentürk
Supervisor, **Chemistry, METU** _____

Examining Committee Members:

Prof. Dr. Ahmet M. Önal
Chemistry, METU _____

Prof. Dr. Emren Nalbant Esentürk
Chemistry, METU _____

Prof. Dr. Ayşen Yılmaz
Chemistry, METU _____

Prof. Dr. Ali Çırpan
Chemistry, METU _____

Prof. Dr. Nurşen Öztaş
Chemistry, Hacettepe University _____

Date: 23.09.2020

I hereby declare that all information in this document has been obtained and presented in accordance with academic rules and ethical conduct. I also declare that, as required by these rules and conduct, I have fully cited and referenced all material and results that are not original to this work.

Name Last name : Rahime Yağmur Ağcalı

Signature :

ABSTRACT

SYNTHESIS AND CHARACTERIZATION OF NICKEL ZINC OXIDE NANOPARTICLES AND THEIR INVESTIGATION AS WATER OXIDATION CATALYST

Ağcalı, Rahime Yağmur
Master of Science, Chemistry
Supervisor: Prof. Dr. Emren Nalbant Esentürk

September 2020, 51 pages

The depletion of fossil fuels has steered attention to discover new energy sources. Fossil fuels are not desirable to use because of their hazardous effects on earth and being non-renewable, yet they have been used as primary energy sources all over the world. Due to their limited amount, the focus of research has become maintaining renewable, green, and clean energy. In this sense, among others hydrogen has a great potential for being a primary source. The possible supplied energy from hydrogen is great and it is clean with no waste. One of the easy ways of producing hydrogen is splitting water. However, half reactions of this process, particularly the anode (water oxidation/oxygen evolution) reaction, are slow and require high energy to proceed. Catalysts can be used to overcome these difficulties. For these reactions, Ru and Ir metals are known as the best catalysts but they are quite expensive and precious. Thus, one of the focus of research in hydrogen production is to synthesize alternative catalysts. For this, heterogeneous metal oxide nanoparticles are gaining great attention due to having high surface area and large numbers of active sites. This thesis study is focused on the synthesis of nickel zinc metal oxide nanoparticles, their characterization by Scanning Electron Microscopy (SEM), Energy Dispersive X-ray Spectroscopy (EDX), X-Ray Diffraction (XRD), X-Ray Photoelectron Spectrometry

(XPS), Brunauer-Teller-Emmet (BET) Isotherm and Transmission Electron Microscopy (TEM) techniques and further, their investigation of electrochemical activities as catalyst in water oxidation reactions.

Keywords: Clean Energy, Nanoparticles, Heterogeneous Metal Oxides, Water Oxidation, Electrocatalyst

ÖZ

NİKEL ÇİNKO OKSİT NANOPARÇACIK SENTEZİ, KARAKTERİZASYONU VE SUYUN YÜKSELTGENME TEPKİMESİNDE KATALİZÖR OLARAK İNCELENMESİ

Ağcalı, Rahime Yağmur
Yüksek Lisans, Kimya
Tez Yöneticisi: Prof. Dr. Emren Nalbant Esentürk

Eylül 2020, 51 sayfa

Fosil yakıtların tükenmeye başlaması dikkatleri yeni enerji kaynakları keşfetmeye yöneltmiştir. Dünya üzerindeki zararlı etkilerinden ve yenilenebilir olmamalarından dolayı fosil yakıtların kullanımı tercih edilmemektedir, ancak dünya genelinde birincil enerji kaynağı olarak kullanılmaktadırlar. Bu kaynakların sınırlı miktarda olması nedeniyle yenilenebilir, yeşil ve temiz enerji kaynağı kullanmak ve kullanımını sürekli hale getirmek araştırmaların odağı haline gelmiştir. Bu bağlamda, diğer alternatif enerji kaynaklarına göre hidrojen, birincil enerji kaynağı olmak için, oldukça büyük bir potansiyele sahiptir. Hidrojenden elde edilecek olası enerji oldukça büyük, ayrıca herhangi bir atık oluşturmadığı için temizdir. Hidrojen üretiminin en kolay yollarından biri suyun ayrıştırılmasıdır. Ancak bu ayrıştırma işleminin yarı reaksiyonları, özellikle anot (suyun yükseltgenmesi/oksijen salınımı) reaksiyonu yavaş ilerleyen ve başlamak için yüksek enerjiye ihtiyaç duyan bir reaksiyondur. Bu zorlukların üstesinden gelmek için katalizörler kullanılabilir. Ru ve Ir metalleri bu reaksiyonlar için bilinen en iyi katalizörlerdir ama oldukça pahalı ve değerlidirler. Bu nedenle hidrojen üretimindeki araştırmaların odak noktalarından birisi, alternatif katalizörler sentezlemektir. Bu amaç için heterojen metal oksit nanoparçacıklar, geniş yüzey alanı ve çok sayıda aktif alana sahip olmaları

nedeniyle, büyük ilgi toplamaktadır. Bu tez çalışması nikel çinko oksit nanoparçacık sentezi, SEM, EDX, XRD, XPS, BET ve TEM teknikleri kullanılarak nanoparçacıkların karakterizasyonunun yapılması ve bu nanoparçacıkların suyun yükseltgenme reaksiyonlarında katalizör olarak elektrokatalitik aktivitelerinin incelenmesi üzerine odaklanmıştır.

Anahtar Kelimeler: Temiz Enerji, Nanoparçacıklar, Heterojen Metal Oksitler, Suyun Yükseltgenmesi, Elektrokatalizör

To my beloved family,

ACKNOWLEDGMENTS

I would like to express my deepest gratitude and thanks to my supervisor Prof. Dr. Emren Nalbant Esentürk for her great guidance, kindness, and encouragement during my master period. I am truly honored to have a chance to work with her.

I would like to thank Dr. Asude Çetin for her help during my laboratory experiences.

I would like to thank Prof. Dr. Ahmet M. Önal for his support during electrochemical measurements.

I would like to express my thanks to Prof. Dr. Ayşen Yılmaz for access to the XRD instrument. Also, I would like to thank her group members for helping and teaching measurements.

I would like to thank the Central Laboratory of METU for their help to take characterization measurements.

I would like to thank Scientific and Technological Research Council of Turkey (TUBITAK) for the financial support under Project No: 117Z384

I would like to express my sincere thanks to Serra Kocabaş and İzel Aksoy for their friendship, enjoyed moments all together in the laboratory, and endless support. Also, I would like to thank all NanoClusMate Research Group members.

Finally, I am truly grateful for having such family who are always there for me and I will always there for them. Especially my parents, Doğan Ağcalı and Nurcan Ağcalı, deserves all the credits. With their love and support, I was strong in bad times in my life.

TABLE OF CONTENTS

LIST OF TABLES

TABLES

LIST OF FIGURES

FIGURES

LIST OF ABBREVIATIONS

ABBREVIATIONS

TMO	Transition metal oxide
XRD	X-Ray Diffraction
FWHM	Full width half maximum
SEM	Scanning Electron Microscopy
EDX	Energy Dispersive X-Ray
TEM	Transmission Electron Microscopy
XPS	X-Ray Photoelectron Spectroscopy
BET	Brunauer – Emmett – Teller
GCE	Glassy Carbon Electrode
NTA	Nitrilotriacetic acid
DMF	Dimethylformamide
ECSA	Electrochemically Active Surface Area
RF	Roughness Factor
LSV	Linear Sweep Voltammetry
CV	Cyclic Voltammetry
CPC	Controlled Potential Coulometry

CHAPTER 1

INTRODUCTION

The need for renewable and sustainable energy sources has been growing in all over the world due to depletion of fossil fuels and their permanent hazardous effects on earth. At this point, using hydrogen as an energy carrier has been gaining great attention.

Hydrogen is very promising as being primary energy source in the world due to ease of production from water, which is also renewable and widely available, being clean, renewable and sustainable.[1] One of the most effective and easy way of producing hydrogen is splitting water electrochemically. Water oxidation and reduction half reactions and their research area have been largely expanding in recent years. Yet, there are obstacles for these reactions particularly for the water oxidation that occurred in anode. In this step, multiple electrons and protons transfer for the reaction results in high energy barrier.[1] This energy barrier can be overcome by applying overpotential.[1] Low overpotential results decrease in the need of energy for the reaction. Thus, it is crucial to lower the overpotential and raising the reaction rate. The basic and most effective solution for this problem is using suitable catalysts with high stability and re-using ability. By considering the importance of hydrogen production for energy, designing, and improving new catalysts systems is vitally important. Research has shown that the most effective electrocatalysts for water oxidation are the metal-oxide nanoparticles.[1] Hence, there is plenty of research in designing new metal-oxide nanoparticles as electrocatalysts.

Ruthenium oxide (RuO_2) and iridium oxide (IrO_2) have been reported as two of the most efficient electrocatalysts up to date. Liu et al. reported particularly good results for RuO_2 with 1.34 V (vs RHE) onset potential and 190 mV overpotential at 10 mA cm^{-2} current density (η_{10}).[2] Yang et al. reported a good catalyst ability of RuO_2 with 1.47 V (vs RHE) onset potential and 255 mV overpotential at η_{10}.[3] Similarly, Lim et al. and Liu et al. reported 331 mV and 271 mV overpotential at 10 mA cm^{-2} current density for RuO_2 respectively with onset potential between 1.45-1.50 V (vs RHE).[4,5] In our study, the activity of RuO_2 nanoparticles was found quite close to the above results by demonstrating 1.45 V (vs RHE) onset potential and 326 mV overpotential at η_{10}. Albeit their high catalytic activity, Ru and Ir are precious metals with high costs and their availability is low. Also, they cannot pursue their activity for a long time i.e. low stability.[1,6-8] Thus, synthesizing metal oxide nanoparticles by using cheap and earth abundant metals and also reaching high stability and activity is a vital and challenging goal to achieve.

Nanoparticles in bimetallic forms are taking great attention due to being quite active as electrocatalysts.[9] Therefore, there are various combinations of bimetallic oxide nanoparticles reported as electrocatalysts in water oxidation.[2-7] As bimetallic oxide nanoparticles, spinels and perovskites were largely reported with good catalytic activities and stabilities in alkaline mediums.[6,10-14]

Nickel-based bimetallic oxides are widely reported as successful electrocatalysts, and also iron and cobalt are other important elements used in the catalyst systems due to being electrically conductive and rich in redox chemistry. These three elements have different combinations with various metals and with each other in the literature. Yuan et al. have studied the tubular ferrite combinations of these three elements in spinel form (MFe_2O_4, M: Fe, Ni, Co) and compared their activity in water oxidation. The comparison was done via overpotentials at 10 mA cm^{-2} current density (η_{10}) and results were revealed as 340, 392 and 432 mV for $NiFe_2O_4$, $CoFe_2O_4$ and Fe_3O_4 respectively, and $NiFe_2O_4$ was found as the most effective combination for this study.[15] Yang et al. also reported $NiFe_2O_4$ as a good electrocatalyst in the form of atomically thin quantum dots with an overpotential of

262 mV at η_{10}.[16] Additionally, Fang et al. measured the oxygen evolution reaction electrocatalytic activity of $NiFe_2O_4$ for nickel foam (NF) and overpotential of $NiFe_2O_4$/NF was reported as 293 mV at the current density of 10 mA cm^{-2}.[17] Another study for Ni and Fe combination was revealed by Liu et al. and in this study the combination of NiO/$NiFe_2O_4$ shown higher activity than NiO and $NiFe_2O_4$.[18] At η_{10} and with 350 ºC calcination temperature, NiO/$NiFe_2O_4$ had 302 mV overpotential while pure NiO and pure $NiFe_2O_4$ had 364 mV and 342 mV, respectively.[18]

Another widely studied combination is Ni-Co oxides. For instance, Elekkiya et al. reported flower like nanoparticles of $NiCo_2O_4$ as an efficient electrocatalyst with 360 mV overpotential at 10 mA cm^{-2} current density (η_{10}).[19] Similarly, Zhu et al. reported Ni-Co_2-O hollow nano sponges as effective water oxidation electrocatalyst with having low onset potential of 1.501 V and overpotential of 362 mV at η_{10}.[20] Moreover, Ni and Co has been studied by coupling W and producing $NiWO_4$ and $CoWO_4$ combinations. Srirapu et al. reported the electrocatalytic activity of $NiWO_4$ and $CoWO_4$ nanosized structures as 388 mV and 507 mV at η_{10}.[21]

Although, Ni, Fe and Co are relatively earth-abundant elements and have reasonable prices and abundances compared to Ru and Ir, their combination with other elements such as Zn, Mn, Cu, Cr can be still cheaper with better or comparable performance. There are some reported studies with these elements. For instance, Fe_2Zn and Fe_2Ni metal organic framework (MOF) were studied as electrocatalysts and overpotentials at η_{10} were found as 1194 mV and 333 mV respectively.[22] This result shows the superiority of the Ni-based material over Zn. Also, $ZnCo_2O_4$ was studied and results demonstrated still lower performance with 1.78 V (vs RHE) onset potential and 570 mV overpotential.[23]

There are some synthesized Ni-Zn based materials for various applications, but water oxidation. Doğan et al. investigated optical, structural, and morphological properties of NiZnO films.[24] They found the crystallite size of the films varying from 37 nm to 21 nm with increasing Ni concentration. Also, the crystallite structure was changed from wurtzite to cubic. Similarly, Kayani et al. studied the NiZnO thin films.[25] They

also investigated structural, optical, and magnetic properties of the films. The crystallite size was found between 35-52 nm. They noted that the films can be used in devices for magneto-optic effects. İskenderoğlu and Güney studied ZnO:Ni thin films.[26] They investigated the effects of Ni doping on ZnO thin films and found the decreasing crystallite size with increasing Ni-doping. These films can be used in photovoltaic and electrochromic devices as conducting layers. Zn doped NiO nanoparticles investigated by Thangamani and Pushpanathan.[27] By conforming the above studies, they have found increasing grain size with increasing Zn concentration. They noted that these nanoparticles can be used in optoelectronic devices of green emission. Vara and Dave investigated NiZnO, CuZnO and CoZnO nanoparticles and their catalytic activities for thermal behavior of ammonium nitrate (AN) based composite solid propellant (CSP).[28] CSP is used as an energy source in solid rockets and AN is the oxidizer agent of CSP. The aim of using catalyst is to fasten the decomposition of AN. By using metal oxide nanoparticles, they have achieved the desired catalytic effects. The most effective catalyst combination was CuZnO. Another study was completed by Kaviyarasan et al. about Ni-ZnO nanocomposites.[29] They have investigated different morphologies of Ni-ZnO nanocomposites such as nanochains, granular and columnar. They used these synthesized nanomaterials for removing environmental pollutants in wastewater and most successful results were achieved with the columnar structure nanoparticles. Yet, there is no reported combination of Ni and Zn as an effective electrocatalyst in literature.

In consideration of these information, this thesis study targets to synthesize nickel zinc oxide nanoparticles as catalyst in water oxidation. Nanoparticles' synthesis was accomplished by hydrothermal method. The characterization of nanoparticles was managed by various analytical techniques. After characterization, nanoparticles were prepared in suitable form to coat on glassy carbon electrode (GCE) to analyze their electrocatalytic activity. Favorably, the synthesized nanoparticles were monitored as highly stable active catalysts comparable to similar structures reported in literature.

In the following sections of the introduction, background information on metal oxides, their synthesis, characterization, and application on water splitting are presented.

1.1 Transition Metal Oxides

Oxides of transition metals, especially the binary compounds, establish one of the most compelling material group. Stability, facile synthesis and distinct structure and composition of transition metal oxides are the reason for taking great attention. Moreover, transition metal compounds have diverse characteristics such as electrical, magnetic, thermal, optical, etc. This diversity is due to the capability of transition metals to have numerous oxidation states with partially filled d-orbitals and electron interactions in these orbitals, and thus ability to form various combinations of compounds with different properties.[30,31]

The formation of transition metal oxides (TMO)s occurs via electron transfer between less electronegative metal atoms and more electronegative oxygen atoms. There can be various forms of transition metal oxides dependently their electron numbers that are lost in d-orbitals. Monoxides (e.g ZnO), dioxides (e.g IrO_2), trioxides (e.g $CaTiO_3$) and higher complex oxides (e.g $NiFe_2O_4$) can be formed with distinguish bonding and crystal structures for each of them. Thus, transition metal oxides need to define with their crystal chemistry to clarify their roles in specific applications.

TMOs crystals have various names depending on their structures such as rock-salt, wurtzite, perovskite, spinels etc. All these structures and further have commonly large oxide ions arranged in cubic or hexagonal close-packed arrays. This results in octahedral and tetrahedral network formation. Also, these oxide networks lead to formation of holes that are occupied by the smaller transition metals.

There are three main types of transition metal oxides.

1.1.1 Monoxides

All the first-row transition metals can form metal oxides except scandium and chromium. In second row transition metals, five metals can form monoxides that are cadmium, niobium, silver, palladium, and zirconium. Mercury located in third row can form monoxides too. The crystallization of the monoxides is mostly in rock-salt structure with close cubic packing (ccp) arrays formed by oxide ions and octahedral holes occupied by transition metal ions (Figure 1.1a). Rock-salt structure has (6,6)-coordination.[30,31]

Wurtzite structure can be formed by monoxides in the cases of deviations due to nonstoichiometry, relocated atoms or deficiencies in atoms. For instance, CoO forms wurtzite structure with hexagonal close packing (hcp) arrays created by oxide ions and tetrahedral holes half-located with metal ions (Figure 1.1b). Wurtzite structure has (4,4)-coordination.[30,31]

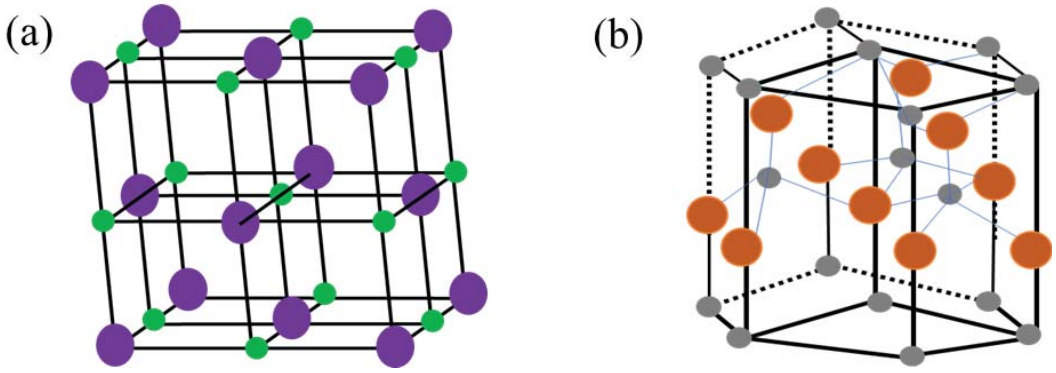

Figure 1.1. (a) Rock salt structure unit cell (purple circles: oxygen atoms, green circles: transition metal atoms). (b) Wurtzite structure unit cell (gray circles: oxygen atoms, orange circles: transition metal atoms)

1.1.2 Dioxides

Titanium, vanadium, chromium, and manganese transition metals from the first row can form dioxides. Except cadmium, other second row and third row transition metals can also form dioxides. Crystal structures of dioxides can be rutile or fluorite. Rutile has hcp arrays formed by oxide ions with empty tetrahedral holes, and transition metal ions occupy half of the octahedral holes (Figure 1.2a). Rutile has (6,3)-coordination.[30,31]

Fluorite structure, on the other hand, has transition metal ions in ccp arrays and oxide ions occupied in tetrahedral holes (Figure 1.2b). The formed lattice has (8,4)-coordination.

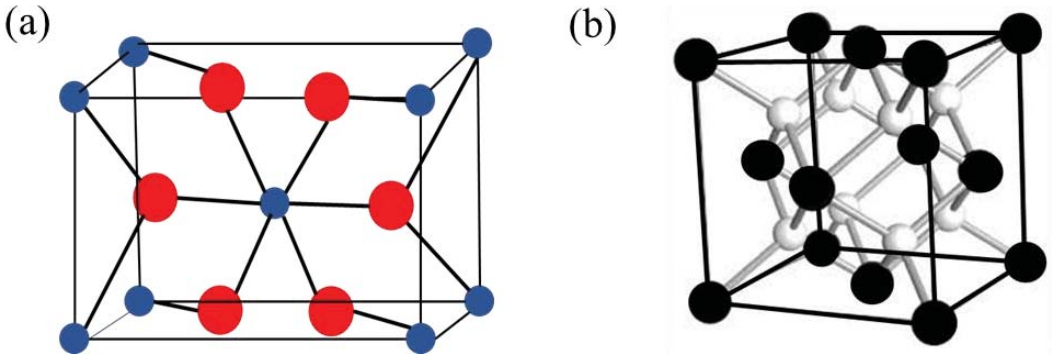

Figure 1.2. (a) Rutile structure unit cell (red circles: oxygen atoms, blue circles: transition metal atoms). (b) Fluorite structure unit cell (white circles: oxygen atoms, black circles: transition metal atoms)

1.1.3 Trioxides

Forming trioxides obligate the +6 oxidation state. Thus, there are limited transition metals forming trioxides. The only transition metals able to form trioxide structures are molybdenum, rhenium, and tungsten. The crystal structure is rhenium trioxide with oxide ions located at the edge of centers and transition metal ions located at the corners (Figure 1.3). Additionally, corner sharing ReO_6 octahedra can be observed.

For instance, layer structure of MoO_3 is constructed by chains of corner sharing MoO_6 octahedral units. The chains connect each other via sharing edge of octahedra and forms double layer.[30]

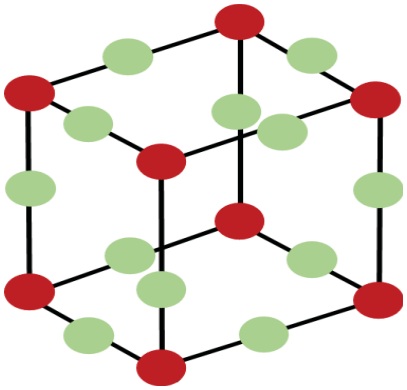

Figure 1.3. Rhenium trioxide unit cell (green circles: oxygen atoms, red circles: transition metal atoms)

1.2 Preparation of Transition Metal Oxide Nanoparticles

In recent years, there is a growing interest toward nanomaterials due to their exclusive properties and activities in countless areas. These valuable abilities of nanomaterials have driven the researchers to seek methods to develop new materials. In the light of research so far, plenty of distinct materials have been synthesized in a wide range of exceptional morphologies with different compositions and crystal structures.

Nanomaterials prepared via transition metal oxides are basically produced by two main paths that are top-down as physical method and bottom-up as both physical and chemical method. Top-down is almost as basic as grinding materials into dust. This minimizing procedure can be pursued by using lithography or related techniques. Yet, the top-down method has some restrictions such as uneven and rough particles collected in atomic scale, non-repeatable procedures and hardly control on desired size of particles.[32] Conversely, by using bottom-up technique, size and shape of

crystallite can be controlled by building blocks such as atoms or molecules or nanoparticles.[32] Additionally, bottom-up technique has a wide range of different methods that are basically named as solid-phase, solution-phase and vapor-phase synthesis.

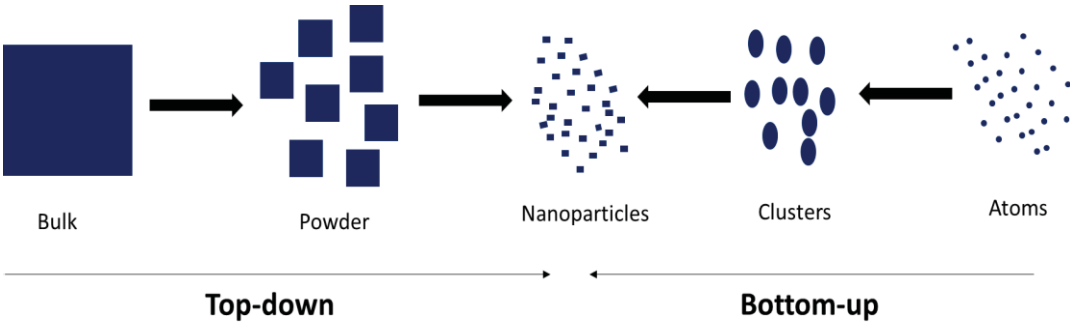

Figure 1.4. Illustration of top-down and bottom-up approaches to synthesize nanomaterials

Solution-phase synthesis is specifically preferred more than solid and gas-phase methods due to being controlled on reaction pathway, facilitating different crystal structure of nanomaterials, uniformity in size distribution, having homogeneous compositions as possible and distinct morphologies.[32] There are commonly used two methods in the solution-phase synthesis of TMO nanomaterials that are named as sol-gel and hydrothermal.

1.2.1 Sol-Gel Method

One of the most used method is sol-gel process as a facile synthesis for metal oxide nanomaterial. It is simply an inorganic polymerization of metal precursors yielding inorganic solids.[6,32] Sol-gel method typically has five steps which are in order as sol formation (metal precursors dissolve in solvent), gel formation (condensation, forming of porous structure), aging (solidification of condensated gel, mostly done by heating), drying (either supercritical drying to form aerogel or thermal

evaporation to form xerogel), and dehydration (thermal treatment, mostly heating to eliminate organic contaminants).

1.2.2 Hydrothermal Method

This is a widely used method to synthesis transition metal oxides with various kinds of morphologies. In this method, water is used as solvent either only or along with other proper solvents such as methanol, ethanol, isopropanol, ethylene glycol etc. This method is a high-pressure solution-phase synthesis and can be classified as solvothermal method.[9] To be able to endure high pressure and temperature, suitable reaction vessels for this method are autoclaves.

After dissolving metal precursor in the solvent as much as possible, the mixture is placed in the autoclave and heated. In this heating process, regions with two different temperatures occur. In the hotter region, precursors dissolve and locate at the bottom of the vessel. Further, the solution moves up the upper part and the cooler part of the solution moves down to the vessel. By lowering the temperature of the upper part, supersaturated solution is obtained where the formation of crystal happens.[33]

This method is quite suitable to control the size and composition of nanomaterials by the modifications on temperature, solvent and also surfactants. Different surfactants such as CTAB (cetyltrimethylammonium bromide), NTA (nitrilotriacetic acid), urea can be used to modify morphologies of nanomaterials.[6]

- Metal precursors
- Surfactant (e.g. NTA, CTAB, urea)
- Water + alcohol

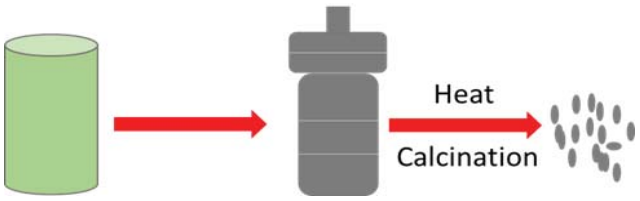

Figure 1.5. Schematic representation of the hydrothermal synthesis procedure of nanoparticles

1.3 Characterization of Transition Metal Oxide Nanoparticles

The as-synthesized nanoparticles are essentially characterized by analytical techniques to clarify whether the nanoparticles are obtained with desired properties or not. The characterization of nanoparticles is focused on the structure, morphology, and composition to have certain information. There are commonly used techniques for the characterization.

Electron microscopy is widely used to detect surface topography, morphology, size and shape of the nanoparticles. Scanning electron microscopy (SEM) provides surface topography analysis, yet it has a lack of resolution to give atomic scale information. Thus, transmission electron microscopy (TEM) is used to reach more detailed information on nanoparticles such as size, shape, composition. Along with SEM and TEM, energy dispersive x-ray spectroscopy (EDX) can be used to have a basic elemental analysis.

X-Ray diffraction (XRD) analysis is also applied to reach the information of crystal structure and chemical composition of the nanoparticles. The material can be also identified by using the characteristic lattice springs sets obtained from x-ray patterns.

Additionally, crystallite size can be determined by XRD with the use of the Debye-Scherrer equation (1.1).[34]

$$\tau = \frac{\kappa\lambda}{\beta\cos\theta} \quad (1.1)$$

where τ is crystallite size, κ is dimensionless shape factor, λ is wavelength (nm) of x-ray, β is the line broadening (radian) at full width half maximum (FWHM) and θ is the Bragg angle.

X-Ray photoelectron spectroscopy (XPS) is applied for the investigation of nanoparticles' surface properties. The emitted photoelectrons from the surface have certain energy levels that expose the chemical and electronic state of the elements in the material and also their concentration and surface distributions. Hence, XPS is quite useful due to providing both quantitative and qualitative information about the surface structure of nanoparticles.

Surface area, pore volume and size along with porosity of the material information can be achieved by adsorption-desorption techniques such as Brunauer-Emmett-Teller (BET) isotherm.

Furthermore, inductively coupled optical emission spectroscopy (ICP-OES), Raman spectroscopy, infrared spectroscopy (IR) and scanning tunneling microscopy (STM) can be utilized as elemental analysis for the further characterization of nanoparticles.

1.4 Water Splitting

Extent usage of fossil fuels has numerous problems for livings and earth itself due to releasing greenhouse gases, not being recyclable and depletion. Consequently, replacing fossil energy sources with renewable and sustainable alternatives gain vital importance recently. Yet, there are some concerns about these new sources such as not being stored efficiently. The most effective solution to this problem is storing the energy of a proper fuel in the chemical bonds.[35]

In this context, hydrogen is taking great attention as an energy carrier and storage. Considering its readily available feature in water and abundance, it is quite promising as a primary energy source. Water splitting is a widely used process to operate formation of hydrogen. The related reactions are summarized in below.[36]

Oxidation half reaction: $2H_2O \rightarrow 4H^+ + O_2 + 4e^-$ (1.2)

Reduction half reaction: $2H^+ + 2e^- \rightarrow H_2$ (1.3)

Overall splitting reaction: $2H_2O \rightarrow 2H_2O + O_2$ (1.4)

Water splitting is a simple way of producing hydrogen, yet the half reactions, specifically water oxidation, have some obstacles by being non-spontaneous $(\Delta G^{\circ} = 475\ kJ/mol)$ with the need for a high amount of energy to occur. This problem can be solved by using the proper catalyst. Water oxidation i.e oxygen evolution occurs naturally in plants. Photosystem II is the oxygen evolution center of plants and this center has a quite effective catalytic activity in water oxidation. The used material as a catalyst in this center is the Mn_4CaO_5 clusters. By consideration of this cluster, researchers have been concentrated on synthesizing new, active, and stable catalysts. Consequently, formation of new catalyst combinations by using transition metals is taking great attention by research in recent years.[37]

There are mainly three types of water oxidation processes that are chemical, photoelectrochemical and electrochemical.

1.4.1 Chemical Water Oxidation

Chemical water oxidation process works with sacrificial reagents to activate transition metals. Water is oxidized by these activated metals to form oxygen. There are several sacrificial reagents such as sodium periodate ($NaIO_4$), hypochlorite (ClO^-), peroxomonosulfate (HSO_5^-) etc. This process is a very quick and easy way of taking information about the performance of catalysts. However, irreversible usage of sacrificial reagents, reducing activity of catalyst and/or transforming it to

another material due to decomposition of reagents by sacrificial reagents, affected catalyst stability by using large amounts of sacrificial reagents are the limiting factors of this process.[38,39]

1.4.2 Photoelectrochemical Water Oxidation

Light is used in this method to activate catalyst and to oxidize water. Catalyst composition can be the composites of metal-semiconductors. By this composite, semiconductor is the photocatalyst and metal part is the co-catalyst.[38] Exposition of light results in electron migration from the valence band of photocatalyst to conduction band and an electron-hole pair occur. The adsorbed water in the positively charged holes is oxidized while reduction of protons occurs via electron transferred to the co-catalyst.

There is also a three-component system with components of molecular catalyst, sacrificial electron acceptor and photosensitizer can be utilized in water oxidation photochemically. Basically, light excites the photosensitizer and results in electron transfer to sacrificial electron acceptor. Then, catalyst is activated by oxidized photosensitizer and consequently, catalytic cycle is started. The obstacle in this process is the possible effects of produced reactive singlet oxygen on the stability of the photosensitizer.[36]

1.4.3 Electrochemical Water Oxidation

In the electrochemical water oxidation, catalysts used as anode material activated with the applied potential. Water molecules are oxidized by this activated catalyst. Although theoretically this water splitting process seems easy, it is difficult to achieve because of non-spontaneity and high need for energy caused by 4 O-H bonds cleavage and O-O bond formation. To lower the energy barrier, to fasten the reaction and to maintain these effects catalysts are essential. To have the net energy obtained from the reaction, overpotential amount after the use of catalysts is vital. Thus, an

effective catalyst must meet two important needs that are low overpotential and high stability.

Electrochemical oxidation is particularly attractive due to parallel working conditions with solar fuel generation cells.[39] Thus, the systems planning to use in photochemical and/or photoelectrochemical water oxidations can be pre-studied with electrochemical water oxidation. Therefore, successful catalysts of electrochemical oxidation are examined as relevant pre-works of studied solar fuel generation cell catalysts.

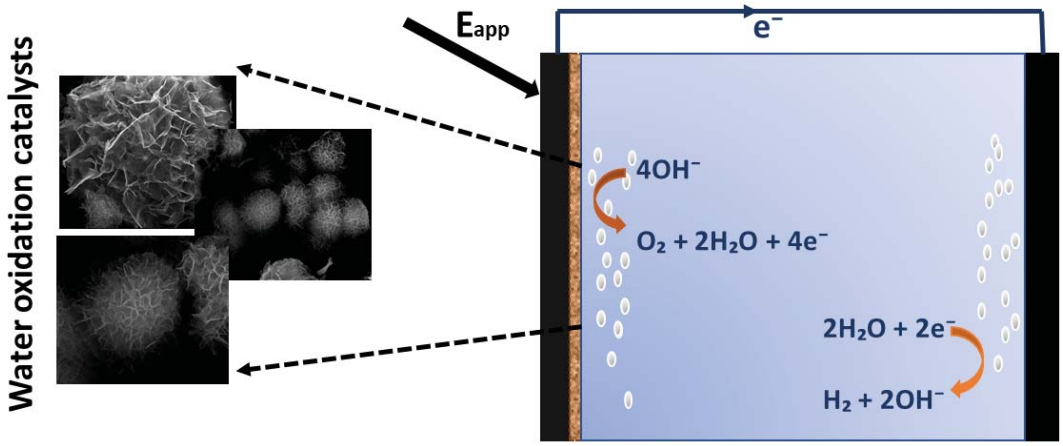

Figure 1.6. Schematic representation of electrochemical water oxidation

1.4.4 Evaluation Parameters of Activity of Water Oxidation Electrocatalyst

Onset potential, overpotential, Tafel slope, capacitance and stability are the most important parameters considered in water oxidation catalysts. These parameters can be achieved by several electrochemical techniques such as linear sweep voltammetry (LSV), cyclic voltammetry (CV), controlled potential coulometry, chronoamperometry etc.

Polarization curves can be resulted from LSVs of studied catalyst modified on the electrode. Onset potential, overpotential and Tafel slope can be evaluated by these curves. *Onset potential* is the potential at which water oxidation starts and in general fits the potential of 10 μA cm^{-2} current density.[6] It can also be obtained from the intersection point of tangent lines; one at the faradaic region where the current density increase is observed while other at the non-faradaic region.[40] Low onset potential refers to effective catalytic activity.

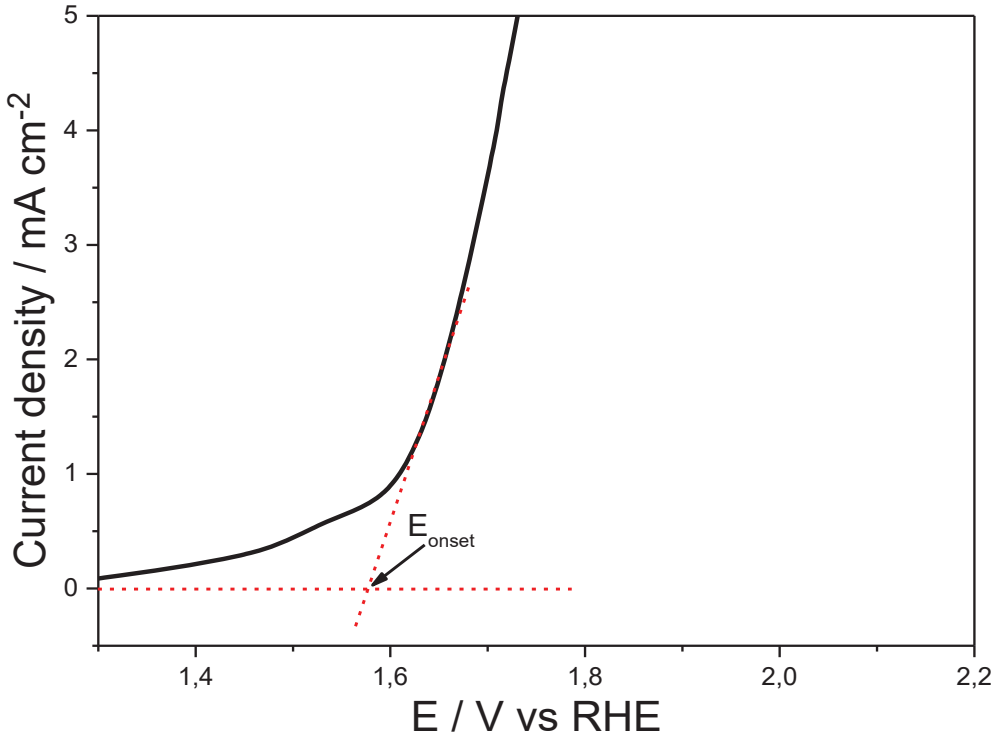

Figure 1.7. Evaluation of onset potential from a polarization curve

Overpotential is the potential difference between applied and equilibrium potential. In an ideal case, these two potentials should be equal. Yet, higher potential than equilibrium potential is used to exceed the reactions kinetic barrier.[6] Overpotential can be found by using the equation given below (1.5). Low overpotential is desired for an efficient electrocatalyst.

$$\eta = E - E_{eq} \quad (1.5)$$

where E is the applied potential and E_{eq} is the equilibrium potential

Tafel slope is another parameter that can be found in polarization curves. Tafel slope can be found by fitting the linear portion of polarization curves to the Tafel equation (1.6). Tafel slope gives information about the mechanism and the rate determining step of the overall reaction.[9] The lower the tafel slope the faster the reaction.

$$\eta = a + b.\log(j_o) \quad (1.6)$$

where η is the overpotential, a is the intercept giving exchange current density j_o and b is Tafel slope.

Double layer capacitance is another parameter which can be determined by electrochemical measurements of catalysts. Double layers form between electrolyte and catalyst film on surface of the electrode and collected charge. By measuring double layer capacitance (C_{dl}), number of atoms act as catalyst can be determined since C_{dl} has a direct proportionality with the active surface area of electrode modified with catalyst. The determination of this C_{dl} value is done by CV measured in a non-faradaic potential region with changing scan rates (v). The recorded current is estimated as double-layer charging current affected (i_{dl}) with the following equation (1.7).[6]

$$C_{dl} = \frac{i_{dl}}{v} \quad (1.7)$$

C_{dl} values of the catalysts are determined as the slope of i_{dl} vs v plot. Additionally, two other important parameters of the catalysts, electrochemical active surface area (ECSA) and roughness factor (RF), can be calculated by using the following equations (1.8) and (1.9), respectively.

$$ECSA = \frac{C_{dl}}{C_s} \quad (1.8)$$

where C_s is the specific capacitance.

$$RF = \frac{ECSA}{GSA} \quad (1.9)$$

where GSA is the geometric surface area of the electrode.

Since the parameters of C_{dl}, ECSA and RF are related to the active surface area of the catalyst, large number of these values imply large number of active sites and consequently, high catalytic performance.

Stability of the catalyst can be determined by applying a constant potential to electrode for a long period of time. Monitoring current density variations during that time is one way to determine stability. If there is almost no change in current density, it declares the good stability of the catalyst. Also, comparison of LSVs before and after the electrolysis gives information about stability. If there is almost no change between the onset potentials and overpotentials of these curves, then catalyst has good stability.

1.5 Motivation of the Thesis Study

World's great energy need and to meet this need by renewable, sustainable, and green sources are in the focus of research. In consideration of energy carrier and storage, hydrogen taking great attention. Hydrogen can easily be obtained from water by water splitting, specifically by water oxidation half reaction. Yet, this process is difficult to pursue both kinetically and thermodynamically due to non-spontaneity and need for high energy to occur. To overcome these problems, using suitable catalysts is the best and easiest way. Hence, developing new catalyst systems for water oxidation reaction has been an attractive research area.

The most effective catalysts with low overpotentials are known as Ru, Ir and their oxides. However, these metals are rare, precious, and highly expensive. Therefore, designing new effective catalyst systems of earth abundant metals with reasonable prices and low overpotentials has been studied widely in all over the world.

Earth abundant metal oxide catalysts have been synthesized with various combinations and morphologies such as line, wire, rod and spherical. Particularly,

nano-sized metal oxides are gaining great attention as active catalysts due to having large active surface areas. In recent studies, bimetallic transition metal oxide nanomaterials have been examined in a broad perspective. The synergistic relations between transition metals and benefits of nano-sized structures lead to very promising results as water oxidation catalysts.

The purpose of this thesis study is to design new catalyst system by synthesizing nickel zinc oxide (NiZnO) nanoparticles and investigating their electrocatalytic activities as water oxidation catalyst. The following studies were completed in this thesis study.

- Synthesis of NiZnO nanoparticles via hydrothermal method.
- Characterization of these synthesized nanoparticles by various analytical techniques that are XRD, EDX, SEM, TEM, XPS and BET.
- Preparation of modified glassy carbon electrode with synthesized nanoparticles.
- Investigation of the electrocatalytic performance of the catalyst in water oxidation reaction.

CHAPTER 2

EXPERIMENTAL

2.1 Materials

All reagents were used as purchased with no further purification. Nickel(II) nitrate hexahydrate ($Ni(NO_3)_2.6H_2O$), zinc nitrate hexahydrate ($Zn(NO_3)_2.6H_2O$), nitrilotriacetic acid (NTA), methyl alcohol, nafion® perfluorinated resin solution (5% wt. in lower aliphatic alcohols and water) and dimethyl formamide (DMF) were purchased from Sigma Aldrich. Deionized ultra-pure water with resistivity greater than 18 MΩ (PURELAB Option-Q, ELGA) was used in the aqueous solutions' preparation.

2.2 Synthesis of NiZnO Nanoparticles

Surfactant stabilized NiZnO nanoparticles were synthesized via hydrothermal method based on a reported procedure in literature with some modifications.[41] Briefly, $Zn(NO_3)_2.6H_2O$ (3.0 mmol), $Ni(NO_3)_2.6H_2O$ (6.0 mmol) and NTA as surfactant (4.7 mmol) were added to 30.0 mL methyl alcohol and 10.0 mL deionized ultra-pure water at room temperature. The prepared solutions were stirred until complete dissolution. The mixture of reaction was placed into a 100.0 mL Teflon lined stainless steel autoclave and kept at 180 °C for 6 h. The reaction product was collected by centrifugation as precipitate and washed with ethanol and ultra-pure water for several times. After washing, the obtained product was calcined at 350 °C for 1 h, and nanoparticles were obtained as grey powder.

2.3 Materials Characterization

Scanning electron microscopy (SEM) images of nanomaterials and energy-dispersive X-ray (EDX) analysis were performed by FEI Nova Nano SEM 430. Transmission electron microscopy (TEM) images were captured from FEI Tecnai G2 F30 electron microscope operating at 300 kV. X-Ray diffraction (XRD) analyses were operated by Rigaku Ultima IV X-ray diffractometer with Cu Kα radiation (λ = 1.54 Å) in the 2θ range from 10º to 80º. X-ray photoelectron spectroscopy (XPS) analyses were carried out on PHI-5000 VersaProbe [Physical Electronics (PHI) Chanhassen, Minneapolis, MN], equipped with Al Kα at 1486.92 eV. The calibration for all data has functioned to the hydrocarbon contamination peak at C1s of 282.4 eV. Brunauer-Emmett-Teller (BET) analysis with Autosorb-6 (Quantachrome Coporation) instrument was performed for the examination of specific surface areas and pore volumes of nanomaterials. Dehydration at 300 ºC for 5 h was carried out for all samples before analyses.

2.4 Electrochemical Characterization

2.4.1 Electrode Preparation

Glassy carbon electrodes (GCE) were used in this study to investigate the characteristics of NiZnO nanoparticles electrochemically. GCEs with 0.07 cm^2 surface area were modified and used in experiments as working electrodes.

Modifications of electrodes were done by consulting the method reported in Kuo et al.[42] In brief, 11.2 mg catalysts were taken and mixed with 2.0 mL DMF, and the solution was sonicated. After 30 min. of sonication., 19 µL nafion® solution was added. The sonication, then, lasted for 2 more hours. At the end, the homogeneous ink-like solution was obtained. 5.0 µL of this solution was planted onto the GCE surface and left to dry in an oven at 90 ºC for 24 h (Figure 2.1). The amount of ink

solution was determined in order to yield 0.4 mg of catalyst mass loading for 0.07 cm^2.

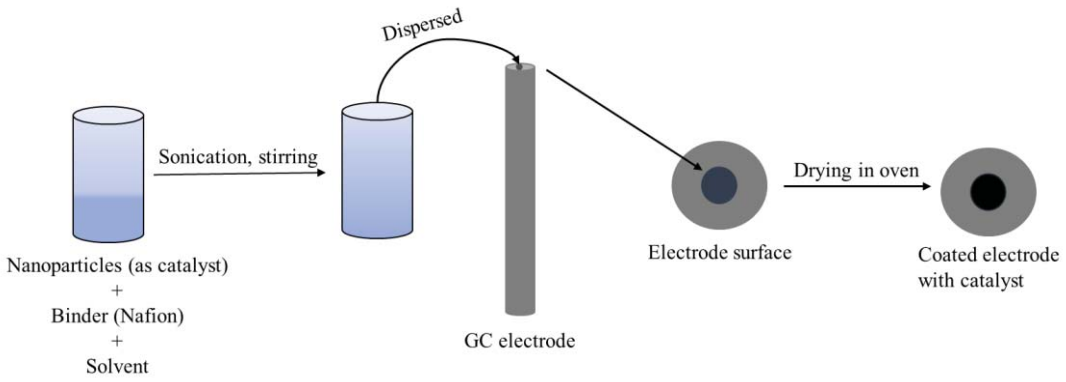

Figure 2.1. Schematic representation of preparation of the modified electrode

2.4.2 Electrochemical Measurement

Gamry 1010B potentiostat-galvanostat and a standard three-electrode system were applied for electrochemical measurements. Counter electrode (CE) was Pt wire, reference electrode (RE) was Ag/AgCl (in 3.0 M KCl) and working electrode (WE) was the coated GCE in this three-electrode system (Figure 2.2).

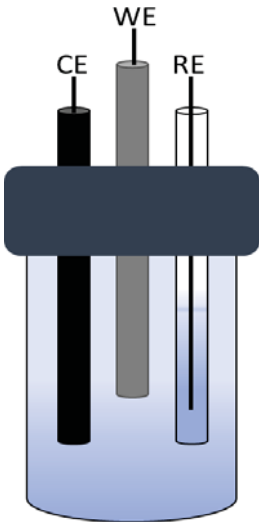

Figure 2.2. Schematic representation of the three-electrode system used for electrochemical measurements

The investigation of the modified electrodes electrochemically proceeded in 0.1 M KOH solution at room temperature. Polarization curves were noted at 5 mV s^{-1} scan rate. All the measured potentials obtained in this study were revised for iR drop and recorded against the reversible hydrogen electrode (RHE). The measured potentials (vs Ag/AgCl) were converted against RHE in accordance with the Nernst equation (2.1) and overpotential (η) was calculated via equation (2.2).

$$E_{RHE} = E_{Ag/AgCl} + 0.059\ pH + E^{o}_{Ag/AgCl} \quad (2.1)$$

$$\eta = E_{RHE} - 1.23\ V \quad (2.2)$$

Linear part of the polarization curves were fitted to Tafel equation (1.6) to exemplify the kinetics of nanoparticles in water oxidation.

The investigation of the stability of the modified GCEs was performed by constant potential electrolysis at certain overpotential in alkaline medium of 0.1 M KOH.

The electrochemical double-layer capacitance (C_{dl}) values were resolved to evaluate the electrochemically active surface area (ECSA) of the catalyst. To determine C_{dl} values, cyclic voltammograms (CVs) were taken at non-Faradaic region of 0.0-0.1 V (vs RHE) for NiZnO catalyst at scan rates of 5-10-15-20-25 mV s^{-1}. The slope of double-layer charging current at 0.1 V (vs RHE) versus scan rate linear plot resulted in the C_{dl} values of the catalyst. The ECSA values were determined by using equation (1.8).

By dividing ECSA of the catalyst to the electrode geometric surface area (GSA) surface roughness factor (RF) was obtained (equation 1.9).

The determination of mass activity (A g^{-1}) values was done by using the equation (2.3) at a certain overpotential.

$$\text{Mass activity} = \frac{j}{m} \quad (2.3)$$

where m (mg cm^{-2}) is the catalyst loading and j (mA cm^{-2}) is the current density.

Specific activity of the catalyst was evaluated by using the equation (2.4).

$$\text{Specific activity} = \frac{i}{ECSA} \quad (2.4)$$

where i is the current observed at a particular potential.

CHAPTER 3

RESULTS AND DISCUSSION

3.1 Surface and Structural Characterization of NiZnO Nanoparticles

Synthesis of NiZnO nanoparticles was performed by the modified hydrothermal method by using NTA as a structure-directing agent. SEM images demonstrate that the synthesized material has spherical-like, porous morphology, which is formed by the assembly of thin flakes (Figure 3.1 a-c). Further analysis by TEM revealed that individual nanoparticles with 14 ± 3 nm size assemble to form nanoflakes (Figure 3.2 a-f). EDX analysis reveal that the nanostructures consist of both Ni and Zn elements (Figure 3.1 d). In addition, EDX mapping on the synthesized material demonstrated that all elements were distributed evenly across the whole material (Figure 3.2 g).

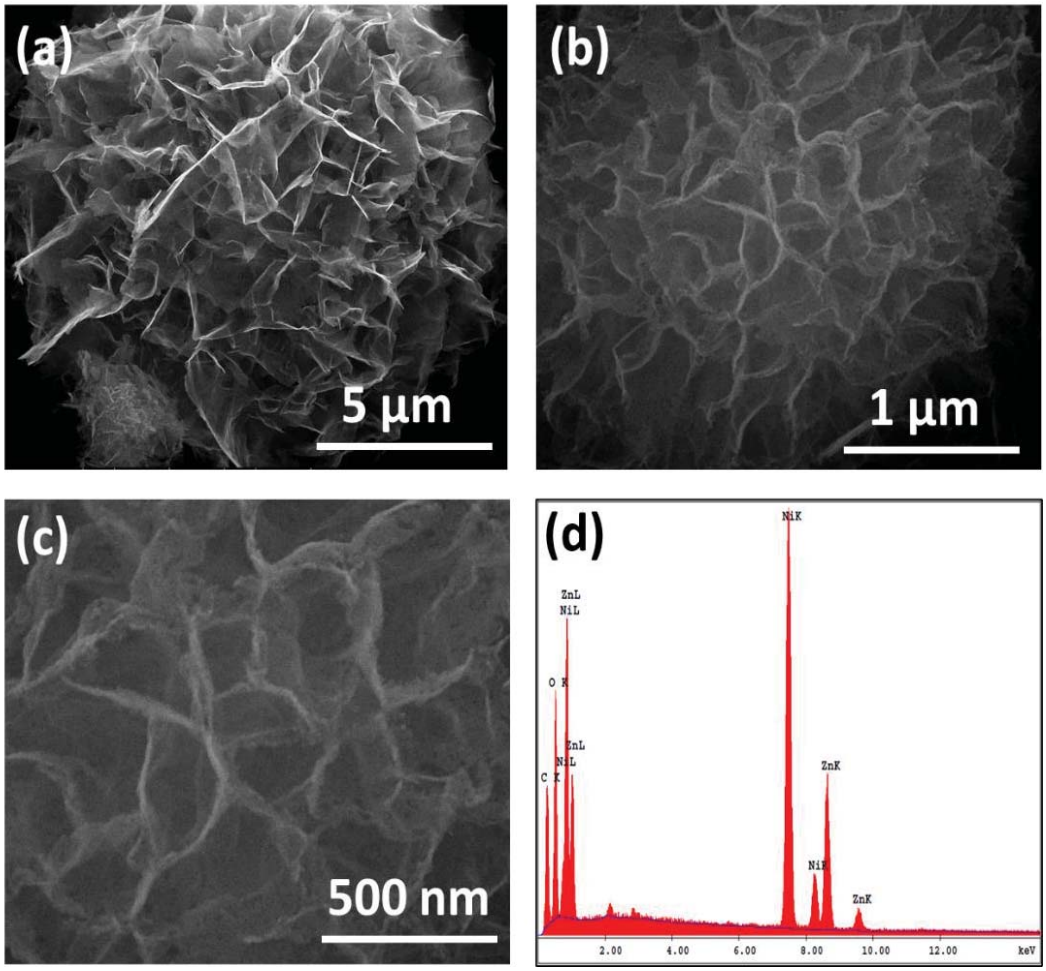

Figure 3.1. (a-c) SEM images and (d) EDX spectrum of NiZnO nanoparticles

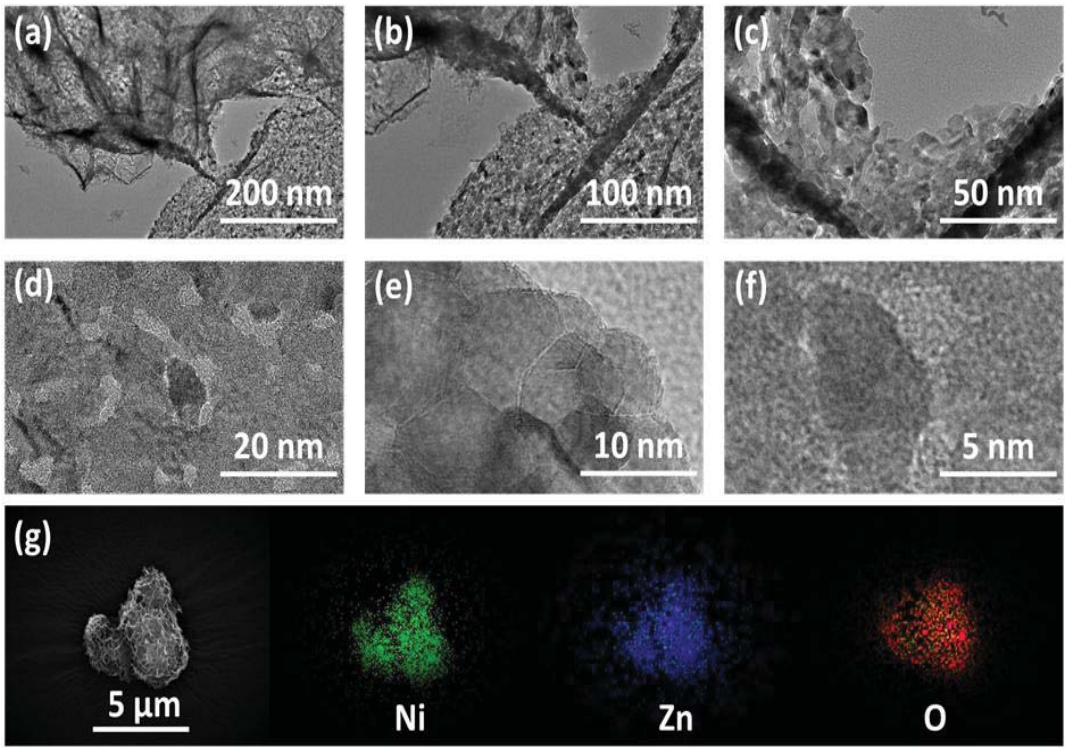

Figure 3.2. (a-f) TEM images at different magnifications and (g) elemental mapping (Ni (green), Zn (blue), and O (red)) of NiZnO

XRD pattern of NiZnO is demonstrated in Figure 3.3. The observed peaks at 2θ values of 31.75º, 34.44º, 47.54º, 56.56º, and 67.92º were assigned to the (100), (002), (102), (110), and (112) planes of $Zn_{0.9}Ni_{0.1}O$ (JCPDS card no: 01-078-3347); 36.92º, 42.90º, 62.26º, 74.64º, and 78.57º were assigned to the (111), (200), (220), (311), and (222) planes of $Ni_{0.8}Zn_{0.2}O$ (JCPDS card no: 01-075-0271) respectively. The probability of $Ni_{0.8}Zn_{0.2}O$ and $Zn_{0.9}Ni_{0.1}O$ structures were estimated as 98% and 24%, respectively. Thus, $Ni_{0.8}Zn_{0.2}O$ was observed as the major product in the synthesized material. The crystallite sizes were estimated by XRD analysis as ca. 7.34 nm. The analysis was performed by evaluating the diffraction peak at 42.90º ((200) plane) by the Debye-Scherrer equation.[24] The size of crystallite is slightly smaller than the size of particles evaluated by TEM.

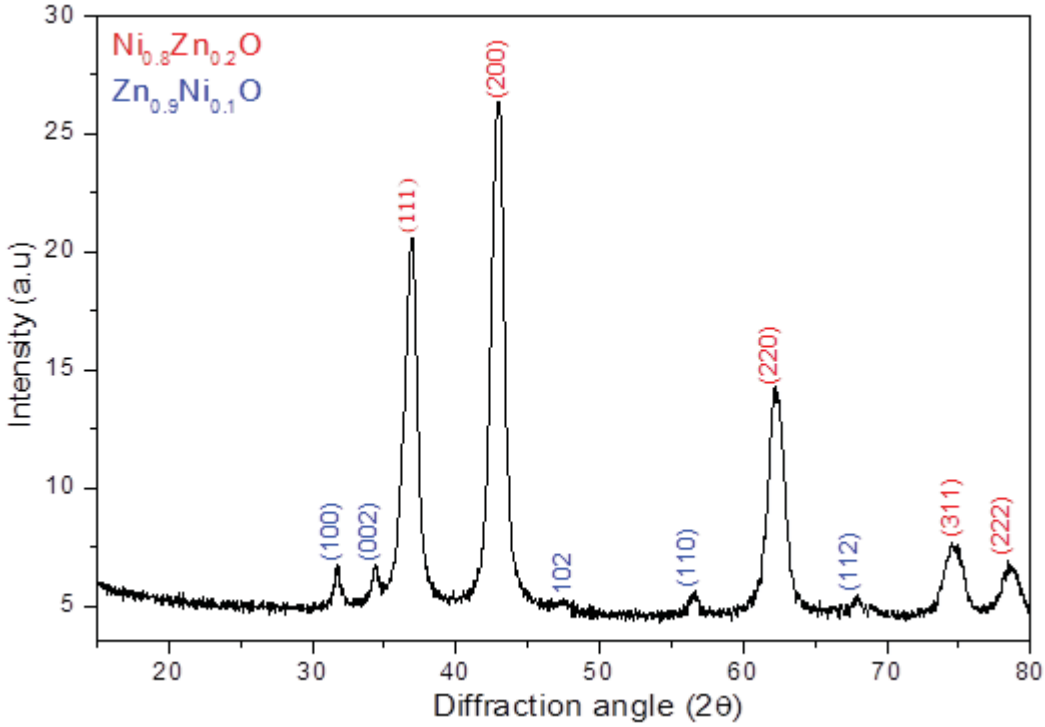

Figure 3.3. XRD pattern of NiZnO nanoparticles (PDF numbers 01-078-3345 and 01-075-0272)

The XPS spectra of the NiZnO nanoparticles are demonstrated in Figure 3.4. In the survey spectrum, the presence of only Ni, Zn, and O elements, except C at 282.4 eV used for calibration, strongly suggests that the as-synthesized material does not contain any impurity (Figure 3.4a). Ni 2p core-level spectrum of the nanomaterials is shown in Figure 3.4b. Corresponding peaks of Ni $2p_{1/2}$ and Ni $2p_{3/2}$ are observed as 870.9 eV, 869.2 eV and 853.8 eV, 851.7 eV respectively. The fitting process resulted in two Gaussian bands that are ascribed to Ni^{2+} (at 870.9 eV and 853.8 eV) and Ni^{3+} (at 869.2 eV and 851.7 eV). These observed peaks and their positions agree well with the ones in previously reported studies.[43,23] In Figure 3.4c, XPS spectrum of Zn 2p is presented. In this spectrum, Zn $2p_{1/2}$ and Zn $2p_{3/2}$ peaks are observed at 1042.5 eV and 1019.4 eV respectively. As expected, these observed peaks are suggesting the presence of Zn in oxidation states of two.[4] O 1s spectrum in Figure 3.4d demonstrates two peaks at 527.1 eV (I) and 529.1 eV (II) that are resolved to

two Gaussian bands. These bands suggest the existence of metal-oxide bonds (peak I) and defect sites with low oxygen coordination (peak II), respectively.[44-48] Oxygen deficient sites are important for having a good catalyst due to adsorption of H_2O molecules on these sites enhancing the effect of catalytic activity.[49,50]

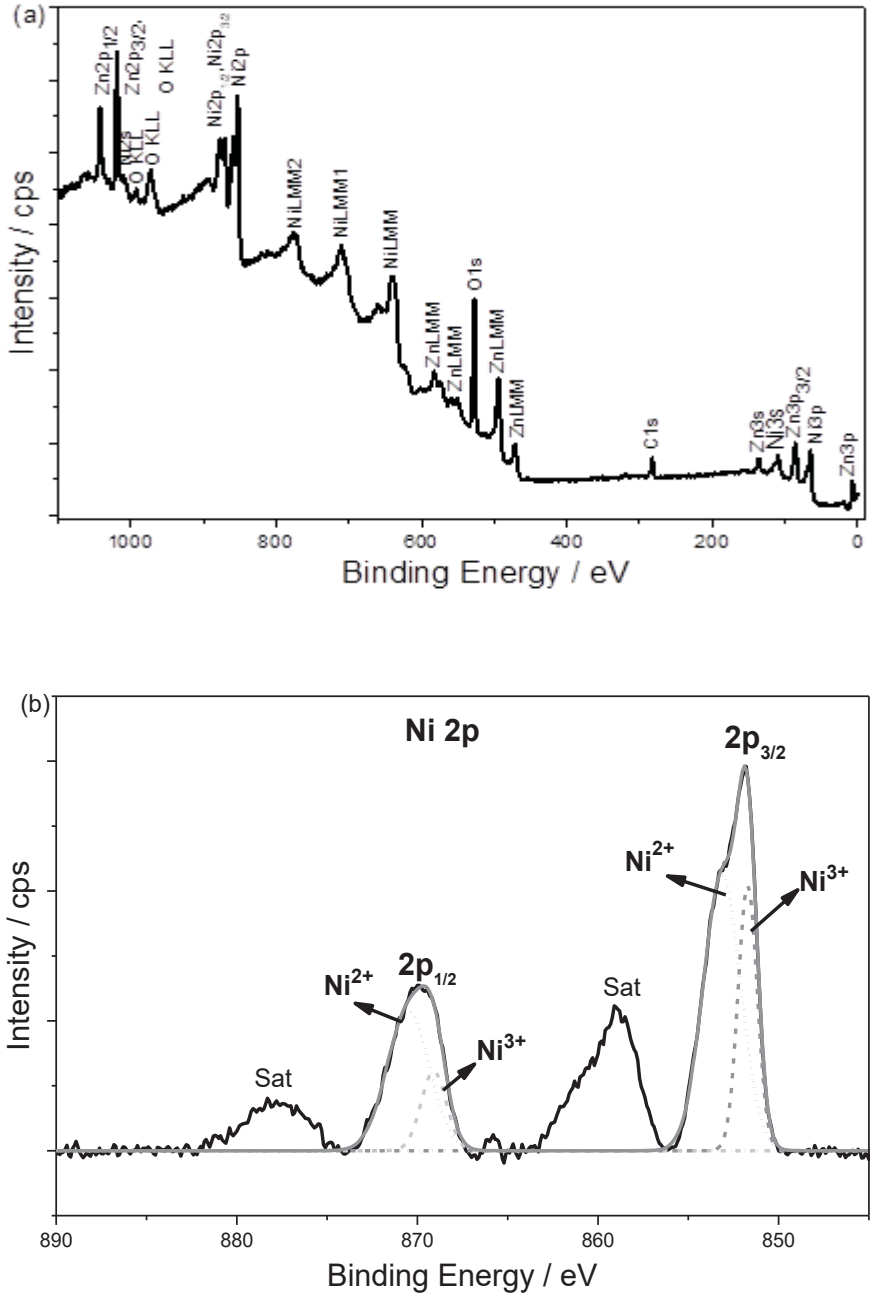

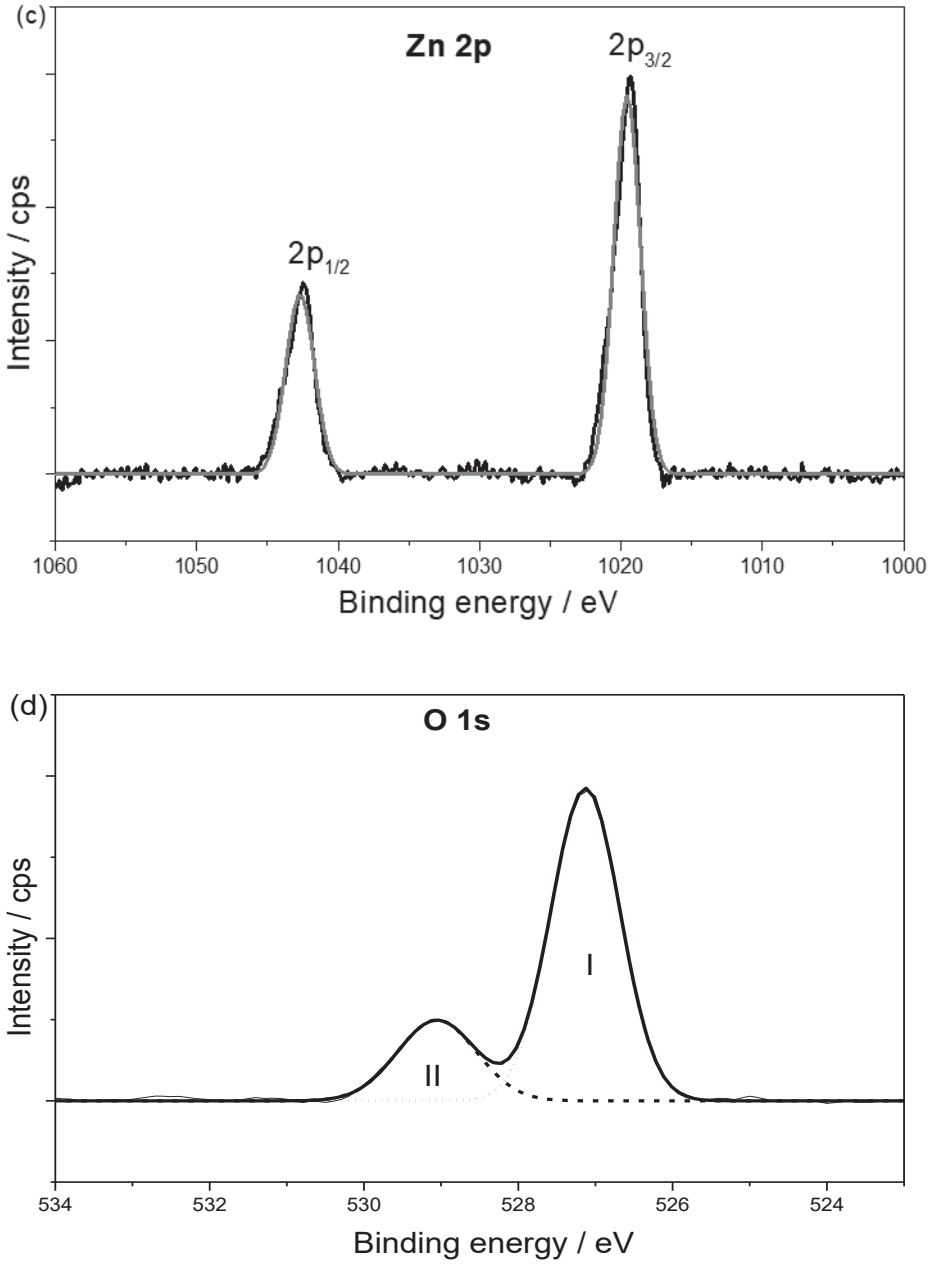

Figure 3.4. XPS (a) survey, (b) Ni 2p, (c) Zn 2p and (d) O 1s spectra of NiZnO nanoparticles

In order to determine the surface area and the pore size of NiZnO nanoparticles, BET analysis was performed. The specific surface area was measured as 72.6 $m^2 g^{-1}$. In addition to that, the presence of a hysteresis loop at relative pressure of 0.4 in

nitrogen adsorption-desorption isotherm suggested that NiZnO nanoparticles have mesoporous structure with a pore size of 3.4 nm (Figure 3.5).[41] To enlarge the interaction spot number and consequently to improve the performance of the catalyst, large surface area and porosity are decisive. BET analysis results showed that NiZnO nanoparticles have large surface area and porosity and thus, good catalytic activity is expected.

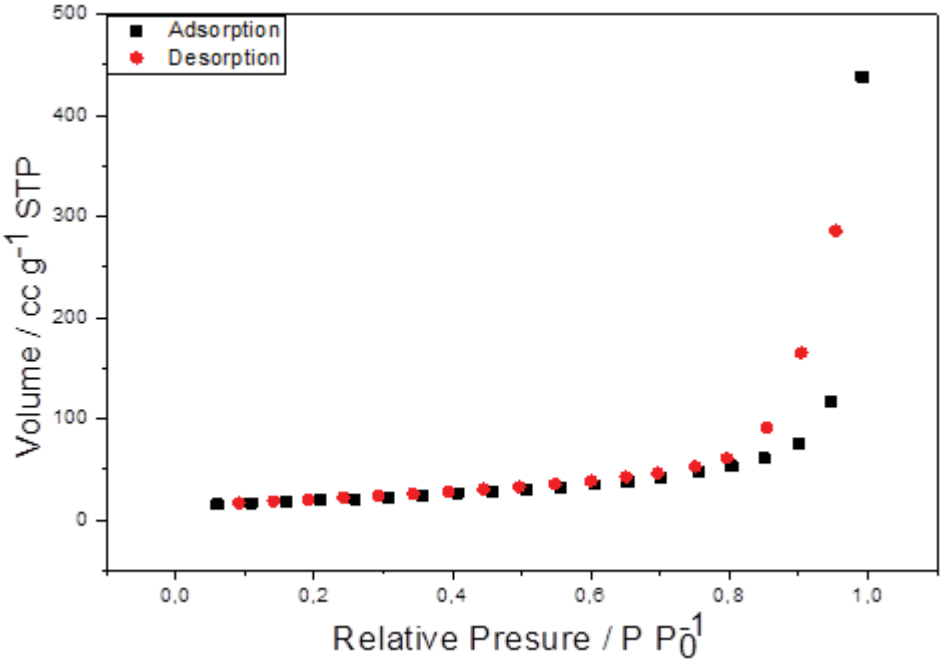

Figure 3.5. BET isotherm of NiZnO nanoparticles

3.2 Electrocatalytic Activity of NiZnO Nanoparticles

The investigation of the electrochemical activity of synthesized nanoparticles for water oxidation was performed in an alkaline medium at room temperature by linear sweep voltammetry (LSV).

In Figure 3.6 a, polarization curves of GCEs modified with NiZnO and RuO_2 as well as bare GCE are given. RuO_2 is the benchmark catalyst for this study since it is known as one of the most efficient electrocatalyst for water oxidation reaction. The onset potential for NiZnO was found as 1.58 V (vs RHE) which is significantly

higher than bare electrode and comparable with RuO_2 (1.45 V vs RHE). It has also comparable or even smaller onset potential than those of previously reported Ni and/or Zn containing catalysts such as NiO nanoparticles (1.59 V vs RHE)[51], Ni-Co-O nanoparticles (1.53 V vs RHE)[51], ZnO nanoparticles (2.22 V vs RHE)[49], $NiCo_2O_4$ nanoparticles (1.63 V vs RHE)[23], $ZnCo_2O_4$ nanoparticles (1.78 V vs RHE)[23].

Another important parameter of electrochemical activity is the required overpotential to produce 10 mA cm^{-2} or higher current densities. NiZnO nanoparticles can reach 10 mA cm^{-2} and 20 mA cm^{-2} current densities with overpotentials of 473 mV and 543 mV, respectively. RuO_2 has better overpotential values than that of NiZnO and can reach to 10 mA cm^{-2} and 20 mA cm^{-2} current densities at 326 mV and 380 mV, respectively. On the other hand, NiZnO has comparable or even better overpotentials than those of previously reported catalysts containing Ni and/or Zn such as NiO nanoparticles (427 mV)[51], $NiCo_2O_4$ nanoparticles (440 mV)[23], Ni-Co-O nanoparticles (410 mV)[51], Fe_2Ni-MOF (metal organic framework) (333 mV)[22], Fe_2Zn-MOF (1194 mV)[22], $ZnCo_2O_4$ nanoparticles (570 mV)[23], $ZnCo_2O_4$ spindle (389 mV)[53], $ZnCo_2O_4$ truncated drum (419 mV)[53].

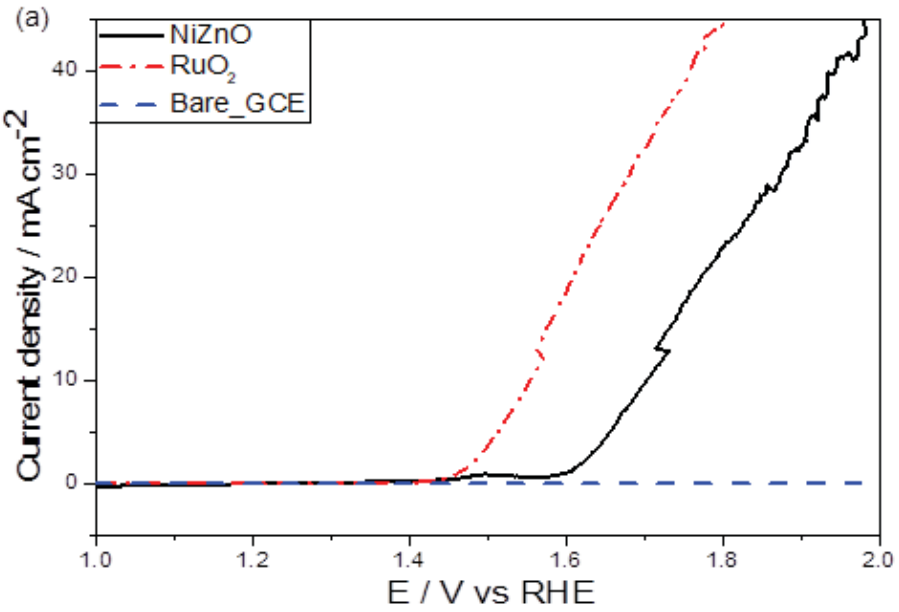

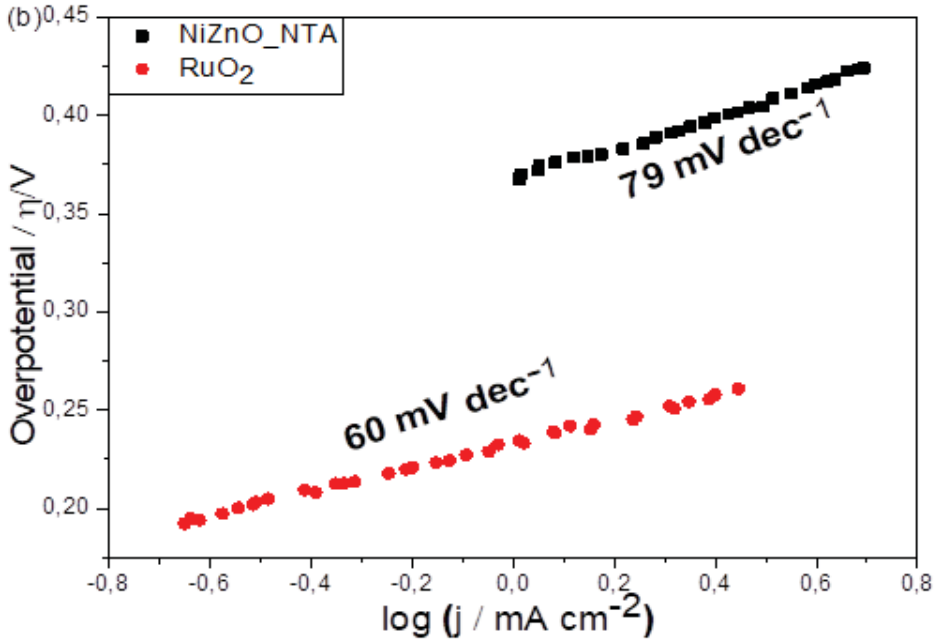

Figure 3.6. (a) Polarization curves of bare CGE, NiZnO nanoparticles and RuO_2 in 0.1 M KOH at a scan rate of 5 mV s^{-1} and (b) their corresponding Tafel plots.

Kinetics of water oxidation reaction of nanoparticles were evaluated by finding Tafel slope. Tafel slope was calculated by the fitting process of linear part of the polarization curves and is giving important information about the catalytic activity. The smaller slope suggests the higher performance of a catalyst. In Figure 3.6 b, the Tafel slopes of NiZnO nanoparticles and RuO_2 are given as 79 mV dec^{-1} and 60 mV dec^{-1}, respectively. Although the Tafel slope of NiZnO nanoparticles is larger than that of RuO_2, it is still comparable to that of RuO_2 and even better than some of the other previously reported catalysts such as NiO nanoparticles (117 mV dec^{-1})[51], $NiCo_2O_4$ nanoparticles (85 mV dec^{-1})[23], Ni-Co-O nanoparticles (71.2 mV dec^{-1})[51], Fe_2Ni-MOF (metal organic framework) (47.8 mV dec^{-1})[22], Fe_2Zn-MOF (330.5 mV dec^{-1})[22], ZnO nanoparticles (245 mV dec^{-1})[52] ,$ZnCo_2O_4$ nanoparticles (135 mV dec^{-1})[23], $ZnCo_2O_4$ spindle (59.54 mV dec^{-1})[53], $ZnCo_2O_4$ truncated drum (70.26 mV dec^{-1})[53]. In Table 3.1, examples of Zn and/or Ni electrocatalysts are given for comparison.

Table 3.1. Summary of some other reported water oxidation catalysts containing Ni and/or Zn and NiZnO nanoparticles

	Onset (RHE)	η10 (mV)	Tafel (mV/dec)	Medium	REF
NiZnO	**1.58**	**473**	**79**	**0.1 M KOH**	**This work**
NiO	1.59	427	117	0.1 M KOH	51
Ni-Co-O	1.52	410	71.2	0.1 M KOH	51
$NiCo_2O_4$	1.63	440	85	1.0 M KOH	23
Fe_2Ni-MOF	-	333	47.8	1.0 M KOH	22
Fe_2Zn-MOF	-	1194	330.5	1.0 M KOH	22
ZnO	2.22	-	245	0.1 M PBS	52
$ZnCo_2O_4$	1.78	570	135	1.0 M KOH	23
$ZnCo_2O_4$ spindle	-	389	59.54	1.0 M KOH	53
$ZnCo_2O_4$ truncated drum	-	419	70.26	1.0 M KOH	53
RuO_2	1.45	326	60	0.1 M KOH	This work

Catalytic activity is also affected by the number of active sites on surface of nanomaterials. The larger the active sites the higher the activity of the catalyst. For this, ECSA and RF values are important since these values are directly related to the number of active sites. By calculating C_{dl}, ECSA value can be obtained. As seen in Figure 3.7, by recording CVs at non-Faradaic potential range with varying scan rates, C_{dl} value can be obtained. Double layer charging current density (at 0.09 V vs RHE) versus scan rate plot's slope results in the C_{dl} value of the catalyst. By applying this procedure, NiZnO nanoparticles' C_{dl} value and ECSA were calculated as 0.947 mF and 15.78 cm^2 respectively. By using ECSA value, RF was calculated as 225. Higher ECSA and RF values imply large active surface area which approves the good catalytic activity of the nanoparticles. Moreover, mass activity and specific activity of NiZnO nanoparticles were determined as 125 A g^{-1} and 0.222 mA cm^{-2}_{ECSA} at an overpotential of 799 mV, respectively. For RuO_2, these values were calculated as 170 A g^{-1} mass activity and 0.237 mA cm^{-2}_{ECSA} specific activity. Mass activity and specific activity of the NiZnO nanoparticles can be considered similar to the ones of RuO_2 suggesting the promising activity of the nanoparticles as an electrocatalyst.

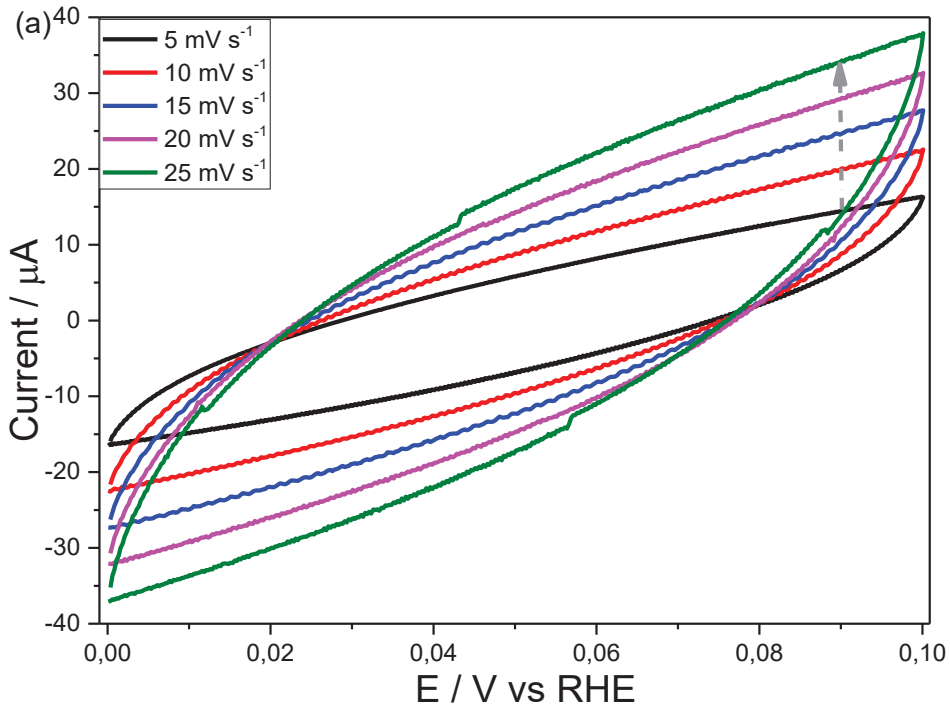

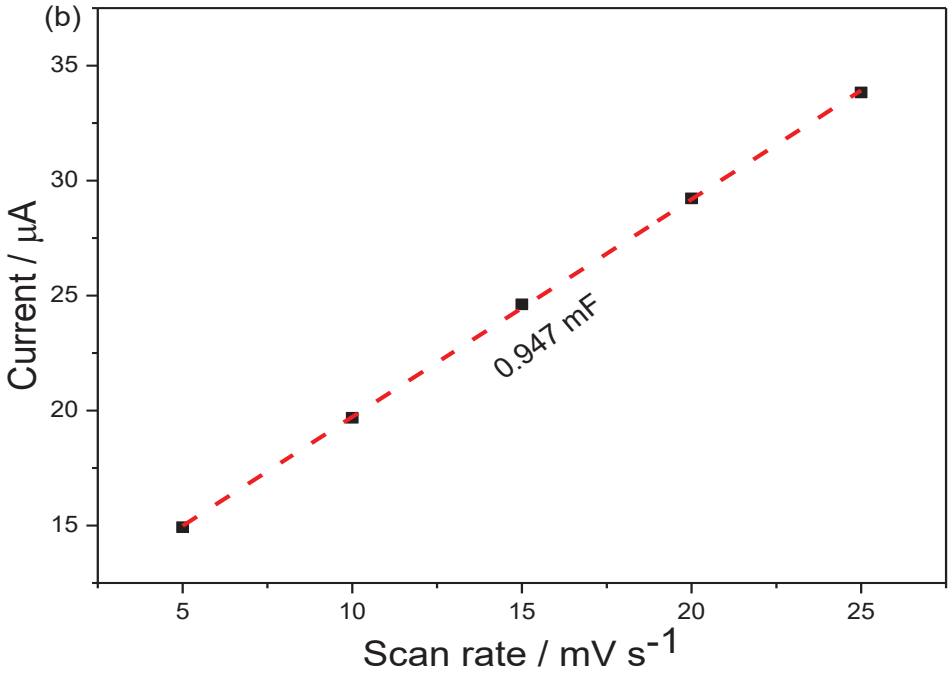

Figure 3.7. (a) CVs of NiZnO nanoparticles taken at various scan rates from 5 to 25 mV s-1 and (b) Plot of current density at 0.09 V (vs RHE) vs scan rate

The stability of the electrocatalyst is also crucial as much as activity. Catalysts are desired to be durable enough for the usage in practical applications. Thus, stability of NiZnO modified electrode was also investigated. To do this, controlled potential electrolysis was performed at an overpotential of 739 mV (vs RHE) for 8 h (Figure 3.8a). It was observed that the catalyst was quite stable for 8 h. Also, linear sweep voltammograms before and after constant potential electrolysis demonstrated only slight changes on overpotentials and no change on onset potential (Figure 3.8 b). The onset potential remained at 1.58 V (vs RHE) after the electrolysis. However, there was an oxidation observed in LSV curve after 8 h CPC. Although the onset potential did not change after the CPC, an oxidation peak appeared at about 1.55 V vs Ag/AgCl (Figure 3.8 b) most probably due to the formation of NiOOH and/or ZnOOH. It is previously reported that in an alkaline medium, Ni^{2+} ion can form NiOOH which is electrochemically active specie.[54,55,56,57] For NiZnO nanoparticles, related reaction with the alkaline medium can be written as in equation 3.1

$NiZnO + 4OH^- \rightarrow NiOOH + ZnOOH + H_2O + 4e^-$ (3.1)

After the oxidation peak, LSV curves remained the same as before CPC. Before and after overpotentials at 10 mA cm^{-2} were estimated as 473 mV and 508 mV, respectively. Considering the very long working time of the electrode, this slight increase in the overpotential can be considered insignificant and does not change the fact that the synthesized NiZnO is a very stable electrocatalyst.

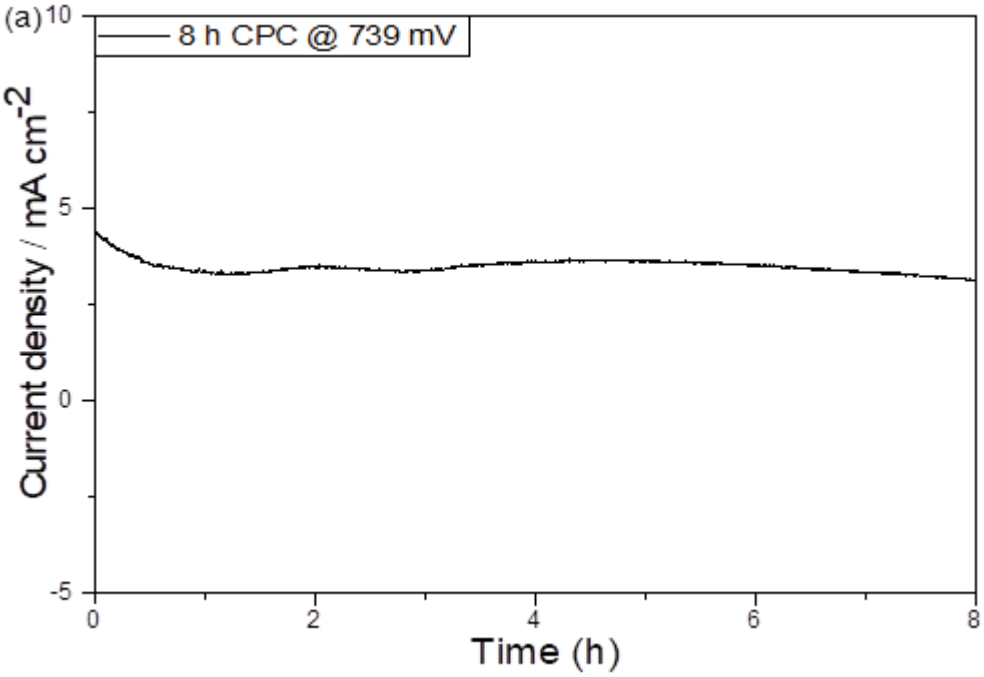

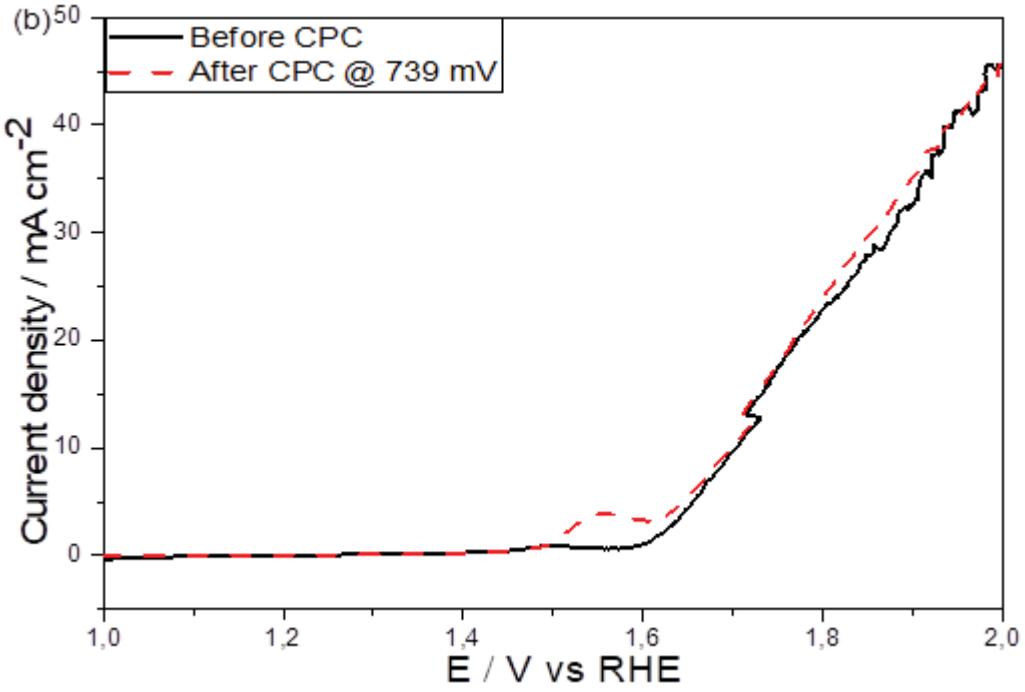

Figure 3.8. (a) Current density changes during controlled potential electrolysis in 0.1 M KOH and (b) Polarization curves of NiZnO nanoparticles obtained before and after electrolysis at overpotential corresponding to initial current density of 5 mA cm^{-2}.

As confirmed in the above results, NiZnO nanoparticles have shown good catalytic activity and thus, it can be considered as a promising electrocatalyst. This desired performance of NiZnO nanoparticles can be linked by their chemical and morphological properties. Having high surface area means increasing activity areas and active sites of the catalyst, thus it is crucial for having a good catalytic activity. As explained in previous parts, both BET analysis and RF, ECSA values approve the large surface area of the NiZnO nanoparticles. Hence, this good catalytic activity of nanoparticles can be linked by their surface area. Moreover, smaller size of nanoparticles results in higher overall surface area and consequently increase in active sites of the catalyst. Also, the structural analysis showed that the nanoparticles have oxygen deficient sites which is important for water oxidation. O 1s XPS spectrum (Figure 3.4 d) shows the low oxygen coordination sites of nanoparticles

which means having oxygen deficient sites. H_2O molecules are adsorbed on the oxygen deficient sites and enhance the catalytic activity.[49,50] Additionally, the possible synergic relation between Ni and Zn can increase the charge transfer in the material and leading to good catalytic activity. All these findings demonstrate that NiZnO nanoparticles are effective and very stable electrocatalyst for water oxidation.

CHAPTER 4

CONCLUSIONS

In this thesis study, the aim was to synthesize Ni-Zn-based bimetallic oxide nanoparticles as electrocatalyst for water oxidation. For this, nanoparticle synthesis was performed by using NTA as a surface directing agent. The characterization of NiZnO nanoparticles with various analytical techniques as TEM, EDX-mapping, XRD, XPS, and BET were operated. On the whole, the synthesized nanomaterials were observed to have hierarchical micro spherical morphology. The microspheres are formed by the assembly of nanoflakes that are also the assembly of individual nanoparticles.

Electrocatalytic activity of the nanoparticles was also investigated. Measurements revealed that the nanoparticles had 1.58 V (vs RHE) onset potential, 473 mV overpotential at 10 mA cm^{-2} current density and 79 mV dec^{-1} Tafel slope.

Another examined parameter was the durability of the catalyst prepared by the synthesized nanoparticles. This is very important for practical applications. For the durability assessment, controlled potential coulometry was performed for 8 hours. The onset potential remained the same while overpotential at 10 mA cm^{-2} was increased from 473 mV to 508 mV. This slight change even after very long electrolysis suggests that NiZnO is very durable catalyst for the oxygen evolution reaction.

Comparison of NiZnO nanoparticles with previously reported catalysts containing Ni and/or Zn reveals that NiZnO nanoparticles have satisfactory performance as an electrocatalyst in water oxidation. This synthesized new material can be considered as an efficient electrocatalyst by being easy to synthesize, containing earth-abundant and affordable elements, and particularly having an outstanding stability.

For further research, activity of the catalysts in hydrogen evolution reaction (HER), oxygen reduction reaction (ORR), metal-air batteries, supercapacitors etc. can be investigated. Also, the reaction mechanism in water oxidation can be examined in detail via computational studies.

REFERENCES

(1) Tahir, M., Pan, L., Idrees, F., Zhang, X., Wang, L., Zou, J. J., & Wang, Z. L. (2017). Electrocatalytic oxygen evolution reaction for energy conversion and storage: a comprehensive review. Nano Energy, 37, 136-157.

(2) Liu, J., Nan, Y., Chang, X., Li, X., Fang, Y., Liu, Y., ... & Ma, J. (2017). Hierarchical nitrogen-enriched porous carbon materials derived from Schiff-base networks supported $FeCo_2O_4$ nanoparticles for efficient water oxidation. International Journal of Hydrogen Energy, 42(16), 10802-10812.

(3) Yang, H., Liu, Y., Luo, S., Zhao, Z., Wang, X., Luo, Y., ... & Ma, J. (2017). Lateral-size-mediated efficient oxygen evolution reaction: insights into the atomically thin quantum dot structure of $NiFe_2O_4$. ACS Catalysis, 7(8), 5557-5567.

(4) 4: Lim, D., Oh, E., Lim, C., Shim, S. E., & Baeck, S. H. (2020). Bimetallic NiFe alloys as highly efficient electrocatalysts for the oxygen evolution reaction. Catalysis Today, 352, 27-33.

(5) Liu, Y., Yang, D., Liu, Z., & Yang, J. H. (2020). Nickel foam supported cobalt phosphate electrocatalyst for alkaline oxygen evolution reaction. Journal of Power Sources, 461, 228165.

(6) Zhao, Q., Yan, Z., Chen, C., & Chen, J. (2017). Spinels: controlled preparation, oxygen reduction/evolution reaction application, and beyond. Chemical reviews, 117(15), 10121-10211.

(7) Osgood, H., Devaguptapu, S. V., Xu, H., Cho, J., & Wu, G. (2016). Transition metal (Fe, Co, Ni, and Mn) oxides for oxygen reduction and evolution bifunctional catalysts in alkaline media. Nano Today, 11(5), 601-625.

(8) Jiao, Y., Zheng, Y., Jaroniec, M., & Qiao, S. Z. (2015). Design of electrocatalysts for oxygen-and hydrogen-involving energy conversion reactions. Chemical Society Reviews, 44(8), 2060-2086.

(9) Sharma, G., Kumar, A., Sharma, S., Naushad, M., Dwivedi, R. P., ALOthman, Z. A., & Mola, G. T. (2019). Novel development of nanoparticles to bimetallic nanoparticles and their composites: a review. Journal of King Saud University-Science, 31(2), 257-269.

(10) Ekebas, E., Cetin, A., Önal, A. M., & Esenturk, E. N. (2019). Magnesium substituted cobalt spinel nanostructures for electrocatalytic water oxidation. Journal of Applied Electrochemistry, 49(3), 315-325.

(11) Kocabas, S., Cetin, A., Önal, A. M., & Esenturk, E. N. (2019). Chromium substituted iron oxide nanowires as affordable electrocatalysts for oxygen evolution reaction. Journal of Nanoparticle Research, 21(7), 143.

(12) Cetin, A., Önal, A. M., & Esenturk, E. N. (2019). Nanowires assembled from iron manganite nanoparticles: Synthesis, characterization, and investigation of electrocatalytic properties for water oxidation reaction. Journal of Materials Research, 34(18), 3231-3239.

(13) Cetin, A., & Esenturk, E. N. (2019). Hierarchical nanowire and nanoplate-assembled $NiCo_2O_4$ –NiO biphasic microspheres as effective electrocatalysts for oxygen evolution reaction. Materials Today Chemistry, 14, 100215.

(14) Aksoy, I., Cetin, A., & Esenturk, E. N. (2020). Hierarchical microspheres of Co_2CrO_4 nanoplates for electrocatalytic water oxidation. Journal of Nanoparticle Research, 22(6), 1-12.

(15) Yuan, F., Cheng, X., Wang, M., & Ni, Y. (2019). Controlled synthesis of tubular ferrite MFe_2O_4 (M= Fe, Co, Ni) microstructures with efficiently electrocatalytic activity for water splitting. Electrochimica Acta, 324, 134883.

(16) Yang, H., Liu, Y., Luo, S., Zhao, Z., Wang, X., Luo, Y., ... & Ma, J. (2017). Lateral-size-mediated efficient oxygen evolution reaction: insights into the atomically thin quantum dot structure of $NiFe_2O_4$. ACS Catalysis, 7(8), 5557-5567.

(17) Fang, Z., Hao, Z., Dong, Q., & Cui, Y. (2018). Bimetallic $NiFe_2O_4$synthesized via confined carburization in NiFe-MOFs for efficient oxygen evolution reaction. Journal of Nanoparticle Research, 20(4), 106.

(18) Liu, G., Gao, X., Wang, K., He, D., & Li, J. (2016). Uniformly mesoporous $NiO/NiFe_2O_4$ biphasic nanorods as efficient oxygen evolving catalyst for water splitting. International Journal of Hydrogen Energy, 41(40), 17976-17986.

(19) Elakkiya, R., Ramkumar, R., & Maduraiveeran, G. (2019). Flower-like nickel-cobalt oxide nanomaterials as bi-functional catalyst for electrochemical water splitting. Materials Research Bulletin, 116, 98-105.

(20) Zhu, C., Wen, D., Leubner, S., Oschatz, M., Liu, W., Holzschuh, M., ... & Eychmüller, A. (2015). Nickel cobalt oxide hollow nanosponges as advanced electrocatalysts for the oxygen evolution reaction. Chemical communications, 51(37), 7851-7854.

(21) Srirapu, V. K. V. P., Kumar, A., Srivastava, P., Singh, R. N., & Sinha, A. S. K. (2016). Nanosized $CoWO_4$ and $NiWO_4$ as efficient oxygen-evolving electrocatalysts. Electrochimica Acta, 209, 75-84.

(22) Gu, M., Wang, S. C., Chen, C., Xiong, D., & Yi, F. Y. (2020). Iron-Based Metal–Organic Framework System as an Efficient Bifunctional Electrocatalyst for Oxygen Evolution and Hydrogen Evolution Reactions. Inorganic Chemistry, 59(9), 6078-6086.

(23) Zhao, Y., Zhou, X., Ding, Y., Huang, J., Zheng, M., & Ye, W. (2016). A study of photocatalytic, chemical, and electrocatalytic water oxidation on ACo_2O_4 (A= Ni, Cu, Zn) samples through doping different metal ions. Journal of Catalysis, 338, 30-37.

(24) Dogan, D. D., Caglar, Y., Ilican, S., & Caglar, M. (2011). Investigation of structural, morphological and optical properties of nickel zinc oxide films prepared by sol–gel method. Journal of Alloys and Compounds, 509(5), 2461-2465.

(25) Kayani, Z. N., Kiran, F., Riaz, S., Zia, R., & Naseem, S. (2015). Dip coated nickel zinc oxide thin films: structural, optical and magnetic investigations. Superlattices and Microstructures, 77, 171-180.

(26) İskenderoğlu, D., & Güney, H. (2017). Synthesis and characterization of ZnO: Ni thin films grown by spray-deposition. Ceramics International, 43(18), 16593-16599.

(27) Thangamani, C., & Pushpanathan, K. (2018). Synthesis and characterization of NiZnO nanoparticles. Inorganic and Nano-Metal Chemistry, 48(2), 131-138.

(28) Vara, J. A., & Dave, P. N. (2019). Metal oxide nanoparticles as catalyst for thermal behavior of AN based composite solid propellant. Chemical Physics Letters, 730, 600-607.

(29) Kaviyarasan, K., Sivasankar, T., Ponnusamy, V. K., & Anandan, S. (2020). Ni–ZnO nanocomposites assembled under various morphologies like columnar, nanochains, and granular structure for removal of pollutants. Materials Chemistry and Physics, 123299.

(30) Ashrit, P. (2017). Introduction to transition metal oxides and thin films. Transition Met Oxide Thin Film Based Chromogenics Devices, 73, 151.

(31) Kung, H. H. (1989). Transition metal oxides: surface chemistry and catalysis. Elsevier.

(32) Niederberger, M., & Pinna, N. (2009). Metal oxide nanoparticles in organic solvents: synthesis, formation, assembly and application. Springer Science & Business Media.

(33) Hutchings, G. (2013). Nanocatalysis: Synthesis and applications. John Wiley & Sons.

(34) Loiha, S., Föttinger, K., Zorn, K., Klysubun, W., Rupprechter, G., & Wittayakun, J. (2009). Catalytic enhancement of platinum supported on zeolite beta for toluene hydrogenation by addition of palladium. Journal of Industrial and Engineering Chemistry, 15(6), 819-823.

(35) Najafpour, M. M., Renger, G., Hołyńska, M., Moghaddam, A. N., Aro, E. M., Carpentier, R., ... & Allakhverdiev, S. I. (2016). Manganese compounds as water-oxidizing catalysts: from the natural water-oxidizing complex to nanosized manganese oxide structures. Chemical reviews, 116(5), 2886-2936.

(36) Singh, A., & Spiccia, L. (2013). Water oxidation catalysts based on abundant 1st row transition metals. Coordination Chemistry Reviews, 257(17-18), 2607-2622.

(37) Bofill, R., García-Antón, J., Escriche, L., & Sala, X. (2015). Chemical, electrochemical and photochemical molecular water oxidation catalysts. Journal of Photochemistry and Photobiology B: Biology, 152, 71-81.

(38) Osterloh, F. E. (2013). Inorganic nanostructures for photoelectrochemical and photocatalytic water splitting. Chemical Society Reviews, 42(6), 2294-2320.

(39) Roger, I., Shipman, M. A., & Symes, M. D. (2017). Earth-abundant catalysts for electrochemical and photoelectrochemical water splitting. Nature Reviews Chemistry, 1(1), 1-13.

(40) Demir, E., Akbayrak, S., Önal, A. M., & Özkar, S. (2018). Nanoceria-supported ruthenium (0) nanoparticles: highly active and stable catalysts for hydrogen evolution from water. ACS applied materials & interfaces, 10(7), 6299-6308.

(41) Sun, C., Yang, J., Dai, Z., Wang, X., Zhang, Y., Li, L., ... & Dong, X. (2016). Nanowires assembled from $MnCo_2O_4$@ C nanoparticles for water splitting and all-solid-state supercapacitor. Nano Research, 9(5), 1300-1309.

(42) Kuo, C. H., Mosa, I. M., Poyraz, A. S., Biswas, S., El-Sawy, A. M., Song, W., ... & Suib, S. L. (2015). Robust mesoporous manganese oxide catalysts for water oxidation. ACS Catalysis, 5(3), 1693-1699.

(43) Wei, B., Wu, J., Mei, G., Qi, Z., Hu, W., & Wang, Z. (2019). $NiCo_2O_4$ nanowire arrays rich in oxygen deficiencies for hydrogen evolution reaction. International Journal of Hydrogen Energy, 44(13), 6612-6617.

(44) Pukazhselvan, D., Nasani, N., Pérez, J., Hortigüela, M. J., Yang, T., Bdikin, I., & Fagg, D. P. (2016). Two step mechanochemical synthesis of Nb doped MgO rock salt nanoparticles and its application for hydrogen storage in MgH_2. international journal of hydrogen energy, 41(27), 11716-11722.

(45) Nagamuthu, S., Vijayakumar, S., Lee, S. H., & Ryu, K. S. (2016). Hybrid supercapacitor devices based on $MnCo_2O_4$ as the positive electrode and $FeMn_2O_4$ as the negative electrode. Applied Surface Science, 390, 202-208.

(46) Silambarasan, M., Ramesh, P. S., Geetha, D., & Venkatachalam, V. (2017). A report on 1D $MgCo_2O_4$ with enhanced structural, morphological and electrochemical properties. Journal of Materials Science: Materials in Electronics, 28(9), 6880-6888.

(47) Zhao, J., Li, X., Cui, G., & Sun, X. (2018). Highly-active oxygen evolution electrocatalyzed by an Fe-doped $NiCr_2O_4$ nanoparticle film. Chemical communications, 54(43), 5462-5465.

(48) Yin, J., Li, Z., Yu, Y., Lv, Y., Song, K., Yang, B., ... & Hu, X. (2019). Facile electrodeposition of MFe_2O_4(M= Co, Fe) on carbon cloth as air cathodes for Li-O2 batteries. Ceramics International, 45(10), 13401-13408.

(49) Cheng, F., Zhang, T., Zhang, Y., Du, J., Han, X., & Chen, J. (2013). Enhancing electrocatalytic oxygen reduction on MnO2 with vacancies. Angewandte Chemie, 125(9), 2534-2537.

(50) Bao, J., Zhang, X., Fan, B., Zhang, J., Zhou, M., Yang, W., ... & Xie, Y. (2015). Ultrathin spinel-structured nanosheets rich in oxygen deficiencies for enhanced electrocatalytic water oxidation. Angewandte Chemie, 127(25), 7507-7512.

(51) Gao M, Sheng W, Zhuang Z et al (2014) Efficient Water oxidation using nanostructured α-Nickel-hydroxide as an electrocatalyst. J Am Chem Soc 136:7077–7084.

(52) Meng, C., Gao, Y. F., Chen, X. M., Li, Y. X., Lin, M. C., & Zhou, Y. (2019). Activating Inert ZnO by Surface Cobalt Doping for Efficient Water

Oxidation in Neutral Media. ACS Sustainable Chemistry & Engineering, 7(21), 18055-18060.

(53) Zhang, J., Zhang, D., Yang, Y., Ma, J., Cui, S., Li, Y., & Yuan, B. (2016). Facile synthesis of $ZnCo_2O_4$ mesoporous structures with enhanced electrocatalytic oxygen evolution reaction properties. RSC advances, 6(95), 92699-92704.

(54) Liang, J., Wang, Y. Z., Wang, C. C., & Lu, S. Y. (2016). In situ formation of NiO on Ni foam prepared with a novel leaven dough method as an outstanding electrocatalyst for oxygen evolution reactions. Journal of Materials Chemistry A, 4(25), 9797-9806.Wang, J., Li, K., Zhong, H. X., Xu, D., Wang, Z. L., Jiang,

(55) Guo, J., Yin, Z., Zang, X., Dai, Z., Zhang, Y., Huang, W., & Dong, X. (2017). Facile one-pot synthesis of $NiCo_2O_4$ hollow spheres with controllable number of shells for high-performance supercapacitors. Nano Research, 10(2), 405-414.Hu, Q.,

(56) Juodkazis, K., Juodkazytė, J., Vilkauskaitė, R., & Jasulaitienė, V. (2008). Nickel surface anodic oxidation and electrocatalysis of oxygen evolution. Journal of Solid State Electrochemistry, 12(11), 1469-1479.

(57) Xu, N., Cao, G., Chen, Z., Kang, Q., Dai, H., & Wang, P. (2017). Cobalt nickel boride as an active electrocatalyst for water splitting. Journal of Materials Chemistry A, 5(24), 12379-123